Ore Geology Reviews 89 (2017) 143–170

Contents lists available at ScienceDirect

Ore Geology Reviews

journal homepage: www.elsevier.com/locate/oregeo

Mineralogical, petrographic and fluid inclusion evidence for the link between boiling and epithermal Ag-Au mineralization in the La Luz area, Guanajuato Mining District, México

Daniel Moncada [a,1], Darcy Baker [b], Robert J. Bodnar [a,*]

[a] Department of Geosciences, Virginia Tech, Blacksburg, VA 24061, USA
[b] Equity Exploration Consultants, Ltd., 1510-250 Howe Street, Vancouver, Canada

ARTICLE INFO

Article history:
Received 7 March 2017
Received in revised form 19 May 2017
Accepted 23 May 2017
Available online 8 June 2017

Keywords:
Guanajuato Mining District
La Luz system
Fluid inclusions
Boiling
Mineral exploration
Epithermal precious metals deposits

ABSTRACT

Theoretical, experimental and observation data provide strong evidence that boiling is the dominant depositional mechanism in many low to intermediate sulfidation epithermal precious metals deposits. Textural and petrographic features that are evidence for boiling in the epithermal environment include the presence of coexisting liquid-rich and vapor-rich fluid inclusions, assemblages consisting of only vapor-rich fluid inclusions, colloform quartz, adularia and bladed calcite. We have examined 213 samples collected from surface outcrops, underground workings and drill cores from the central part of the La Luz vein system in the Guanajuato mining district, Mexico. In each sample, the various features that are evidence of boiling have been recorded. These observations have been quantified using a Boiling Confidence Factor that provides a means of scoring and rating each sample or area relative to the likelihood that boiling occurred.

Homogenization temperatures of liquid-rich fluid inclusions within assemblages of coexisting liquid-rich and vapor-rich fluid inclusions have been measured to estimate the depth of trapping of the inclusions, and these data have been used to estimate the depth to the 300 °C isotherm along the La Luz vein system.

Fluid inclusions and mineral textural features show strong evidence of boiling in the deepest levels sampled in the La Luz system. This observation suggests that the bottom of the boiling zone is at some depth beneath the deepest levels explored and opens the potential for additional resources at depth.

1. Introduction

Our understanding of the physical and chemical processes associated with formation of epithermal precious metals deposits has advanced significantly through a combination of studies of well-characterized deposits (Buchanan, 1979; Vikre, 1985; Mancano and Campbell, 1995; Rowland and Simmons, 2012) and their modern analogs, the continental geothermal systems (Browne, 1978; Henley, 1985; Brown, 1986; Person et al., 2008), combined with laboratory (Stefánsson and Seward, 2003; Stefánsson and Seward, 2004) and theoretical (Pokrovski et al., 2014) studies of the ore-forming process. It is now well established that epithermal deposits represent fossil equivalents of continental geothermal systems, and form in the near-surface portion of large magmatic-hydrothermal systems associated with arc volcanism (Hedenquist and Lowenstern, 1994; Simmons et al., 2005; Saunders et al., 2014). Studies also document that precious metals are typically deposited at <300 °C (White and Hedenquist, 1995; Simmons et al., 2005; Bodnar et al., 2014) and depths <1.5–2.0 km (Simmons et al., 2005), and that boiling or fluid immiscibility is commonly associated with precious metal deposition (Buchanan, 1981; Vikre, 1985; Brown, 1986; Clark and Williams-Jones, 1990; Hedenquist et al., 2000; Simmons et al., 2005). In many, but not all, deposits, the bottom of the ore zone coincides with the bottom of the boiling zone (Albinson et al., 2001; Albinson and Rubio, 2001; Camprubi and Albinson, 2007), and in those deposits where boiling is the depositional mechanism there is a sharp cutoff in grade at depths beneath the boiling zone. Gold and silver grades also drop off rapidly upwards from the bottom of the boiling zone, whereas in deposits in which metal deposition is the result of cooling and/or fluid mixing, the grade gradually decreases both upward and downward from the zone of highest grades.

* Corresponding author.
E-mail address: rjb@vt.edu (R.J. Bodnar).
[1] Current address: Department of Geology and Andean Geothermal Center of Excellence (CEGA), Universidad de Chile, Plaza Ercilla 803, Santiago, Chile.

http://dx.doi.org/10.1016/j.oregeorev.2017.05.024
0169-1368/

In this study, we first summarize the abundant data that are available that document the close association between boiling and mineralization in the epithermal environment. Then, we describe mineralogical, textural and fluid inclusion characteristics that provide evidence for the former presence of boiling fluids in the La Luz vein system in the Guanajuato district, Mexico, and their variation both laterally and with depth in the system.

2. Location and geological setting

The Guanajuato mining district is located in the state of Guanajuato (meaning "hill of frogs" in Tarascan, or P'urhÉpecha) in central Mexico, approximately 330 km NW of Mexico City (Fig. 1). The silver ± gold ores occur along three sub-parallel NNW trending vein systems named, from NW to SE the La Luz, Veta Madre and Sierra vein systems (Fig. 1). Mining activity on the La Luz system has passed through a number of boom and bust cycles during its long history. While no records remain of early work in the area from 1548 until 1793 (Velazquez, 1973), numerous operators have worked the La Luz system since 1793. Pre-20th century activity in the La Luz area is summarized by Ward (1828), Blake (1902), Martin (1906), Church (1907a,b), and Botsford (1910). Details on the more recent history can be found in Velazquez (1973).

The Guanajuato Mining District is located in the Mesa Central, an elevated plateau of Cenozoic volcanic and volcaniclastic rocks located in central Mexico (Nieto-Samaniego et al., 2005). The plateau is bounded to the north and east by the Sierra Madre Oriental, to the west by the Sierra Madre Occidental, and to the south by the Trans-Mexican Volcanic Belt. The Guanajuato District is located on the eastern side and at the southern end of the Sierra Madre Occidental province that is composed dominantly of Tertiary volcanic rocks. Cretaceous volcanic rocks underlie the La Luz area and mineralization is thought to have occurred in the Oligocene (Gross, 1975).

Mineralized veins are hosted by the Esperanza Formation and by pillow basalts and andesites of the La Luz Formation that unconformably overlies the Esperanza Formation. The oldest (historical) stopes on the La Luz vein system are located in the northern part of the area and mineralized veins have been reported to be up to 3 m thick, 30 m long and 18 m high. The older stopes lie 12–15 m laterally from the main La Luz vein and were found by following smaller veins (ramaleos, or stringers) that extend away from the main structure (Blake, 1902; Church, 1907b). Some of the stopes are opened to the surface (indicating that mineralization likely extended to the surface), but economic mineralization typically begins ~60 m below the surface (Church, 1907b). A recent drilling program identified previously unrecognized mineralized veins that are up to 600 m long and hosted in the La Luz basalts, with mineralization occurring over a depth interval of 100 m. The average silver grades range from 55 to 177 g/t; average gold grades range from 1.2 to 2.5 g/t (Lewis et al., 2011; Waldegger, 2012).

The La Luz area was examined intermittently by various companies during the past century, but in general there has been little exploration activity and most effort has been focused on under-

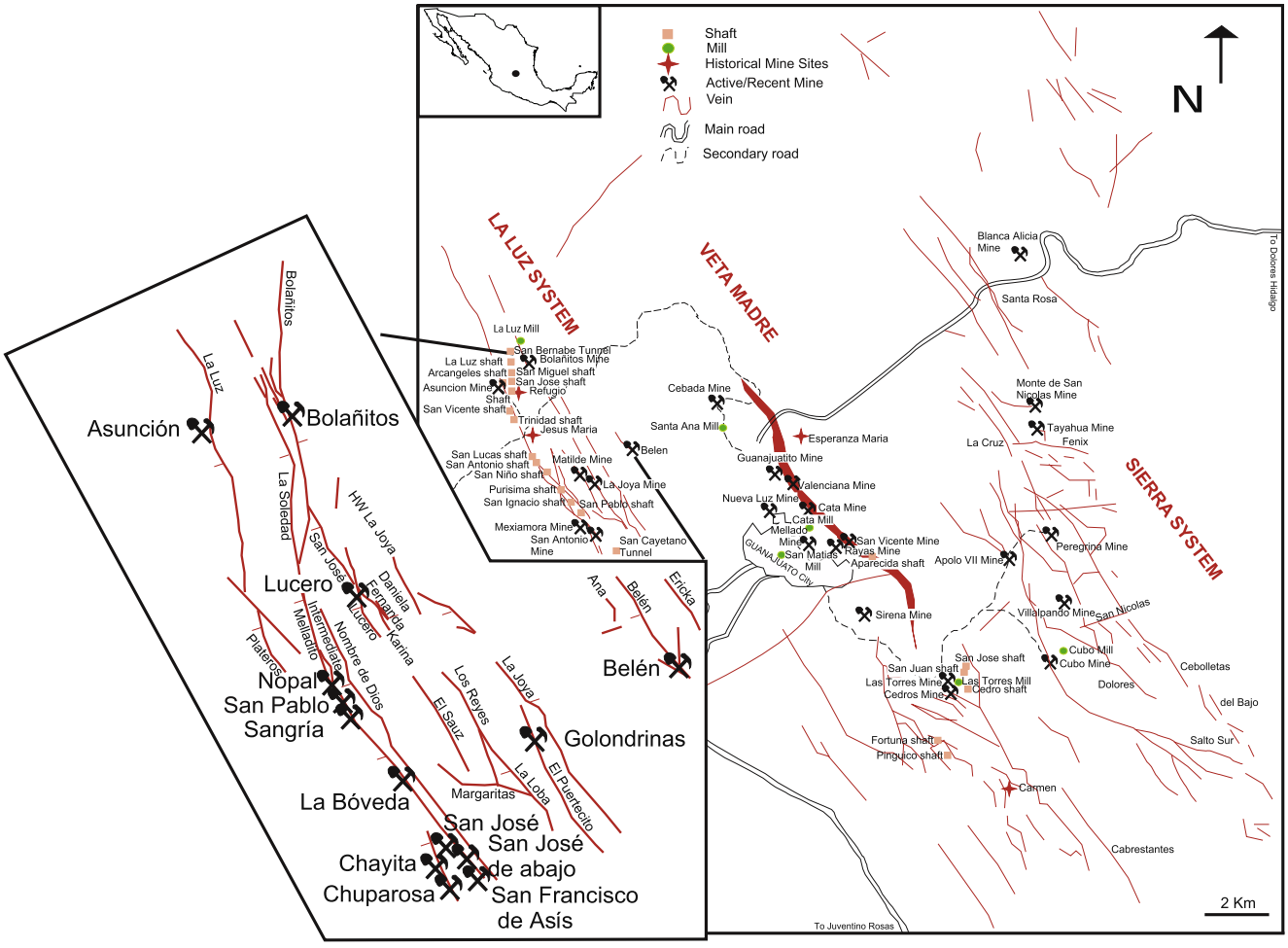

Fig. 1. Location map of the Guanajuato Mining District, Mexico, showing the Veta Madre, La Luz and Sierra vein systems, along with historic and recent mines. An enlargement showing veins and mines on the La Luz system is shown on the left.

ground production (Gómez, 1963; Velazquez, 1973). The mineralized veins are variably associated with argillic, phyllic and propylitic alteration of the wallrocks, and silicification of the vein walls is associated with mineralized veins. The reader is referred to Buchanan (1980) for a more detailed description of the alteration zoning in the Guanajuato district. Mineralized veins usually contain adularia and illite, whereas epidote is found associated with unmineralized veins. The surface expression of veins in the area varies greatly. Some veins, such as the Bóveda vein, are up to two meters wide at the surface and associated with phyllic alteration of adjacent wallrocks, whereas others pinch to the centimeter scale at the surface and are associated with minor argillic alteration.

3. Tectonic history and structural setting

Structural controls have played an important role in the development of the ore deposits in the La Luz area, and Starling (2008) summarized the tectonic and structural history in the La Luz area. Pre-mineralization deformation in the area occurred during the Laramide orogeny (~80–40 Ma) with two main phases; a NE-SW to ENE-WSW compression event followed by a change to NE directed compression. Mineralization in the area is associated with two different extensional events that occurred over a short period of time at ~30–28 Ma, resulting in two stages of mineralization. Early mineralization is associated with anticlockwise motion along the main structures, and secondary mineralization is associated with the Basin and Range style deformation that reactivated earlier structures (Nieto-Samaniego et al., 2005; Starling, 2008). This resulted in structural and hydrothermal telescoping, along with pinching of the ore shoots from changes in dip and/or strike. Starling (2008) suggests that, because of this structural evolution, there is potential to find blind, shallow ore bodies as well as mineralized zones below barren horizons. This interpretation was one of the motivations for recent exploration activity in the La Luz area.

The veins that host mineralization in the La Luz area generally strike 315–360° (NW-SE) and are steeply dipping, and individual veins extend along strike 1.0–3.5 km. A second set of unmineralized veins with a strike of 240° and oriented perpendicular to the mineralized veins is also prominent in the area (Baker, 2011). These veins contain mostly calcite and zonal or comb quartz as described below in the section on paragenesis.

As part of the fieldwork associated with this study, five types of veins were recognized that define a systematic vein paragenesis and textural relationships (Fig. 2). Calcite veins related to early metamorphism or compressional deformation are earliest. These are followed by calcite-epidote veins, with epidote possibly related to sub-greenschist facies metamorphism and unrelated to precious metal deposition. Quartz-pyrite ± calcite stockwork veins are the next youngest vein type, and these locally contain traces of gold with minor silver. These veins in some cases show stockwork within a breccia fragment, indicating multiple stages of brecciation. The next vein type in the paragenesis contains bladed calcite – colloform quartz – pyrite – sulfosalts, shows the highest silver values, and is related to the second extensional event described above. Finally, the paragenesis ends with amethyst and zonal or comb quartz ± rhombohedral calcite veins representing the final hydrothermal event in the La Luz area. The paragenesis and vein descriptions were used as the basis for collecting samples in the field for petrography and fluid inclusion studies described below.

4. Sample collection and methodology

A total of 213 samples were collected from surface outcrops, underground workings, and drill core from the La Luz area. Underground sampling was conducted in several active and inactive historical mines. From north to south, active mines sampled include Bolañitos, San José, Lucero, Karina and Daniela, and inactive historical mines sampled include Nopal, San Pablo, Sangria, La Bóveda, San José, Chayita, San José de Abajo, Chuparosa, San Francisco de Asís, and Belén (Fig. 1). Drill core samples were available only from the central part of the La Luz area and include DDH-1, DDH-4, DDH-9, DDH-14, DDH-17 and DDH-21. These drill holes cut the Melladito, Intermediate and Nombre de Dios veins. Two drill holes, DDH-9 and DDH-14, intersect three different veins, the Melladito, Intermediate and Nombre de Dios veins, at approximately the same depth (but at slightly different locations laterally along the vein). Drill holes LC-03, LC-26, LC-29, LC-31, LC-20, LC-15, DN-1, DN-2, and KA-15 cut the Lucero, Daniela and Karina veins. The Karina and Daniela veins were intersected at different depths by various drill holes, and we have examined metal grades and evidence of boiling at these different depths in section 28600 to characterize the vertical distribution of these features within the vein to better understand the potential for additional resources at depth. Traverses perpendicular to the main veins were conducted on the surface and samples were collected from veins ranging from ≈1 to 20 cm wide.

After sampling, one-half of each sample was analyzed for metals. All samples were analyzed for Au, Ag, but not all samples were analyzed for Cu, Zn, Pb, Sb, and As (Table A1). A thin section was prepared from the other half of the sample for petrographic study to characterize mineral textures, identify ore and alteration minerals, and to examine the fluid inclusions. All data for each sample, including sample number, UTM coordinates, elevation, vein identification, collection location (surface, mine, drill core), concentrations of Au, Ag, Cu, Pb, Zn, As, and Sb, and the various textural and fluid inclusion features observed are listed in Table A1. Note

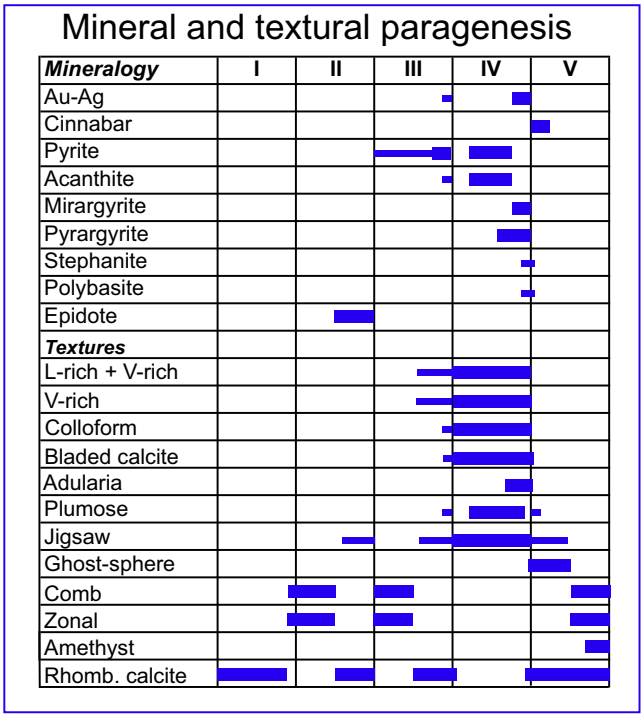

Fig. 2. Mineral and mineral texture (fluid) paragenetic sequence of the La Luz system veins. Note that features associated with boiling, including coexisting liquid-rich and vapor-rich fluid inclusions (L-rich + V-rich), Fluid Inclusion Assemblages containing only vapor-rich fluid inclusions (V-rich), colloform quartz, bladed calcite, and adularia are most common in stage IV, which is also the silver ± gold ore stage.

that the UTM coordinates have been modified from true values at the request of mine operators and land holders.

5. Boiling in the epithermal environment

Our assessment of the exploration potential in the La Luz area is based on the assumption that precious metal deposition in the La Luz area is controlled dominantly by boiling. As such, it is appropriate to review the variety of data that support the assumption that boiling is a common feature in the epithermal environment, and that boiling is the mechanism that often controls gold and silver precipitation.

5.1. Boiling as the depositional mechanism

Abundant theoretical, experimental and observational evidence suggests that boiling is an effective depositional mechanism for gold and silver in the epithermal environment (Seward et al., 2014). Based on experimental results, Stefánsson and Seward (2004) reported that when gold is transported as sulfide complexes, "*Excessive boiling of both dilute and saline geothermal water leads to quantitative loss of gold from solution*". Similarly, using the abundant data available for compositions of fluids in active geothermal systems combined with newly obtained thermodynamic data, Stefánsson and Seward (2003) report that "*Adiabatic boiling of dilute and saline geothermal waters at Ohaaki-Broadlands, New Zealand and Reykjanes, Iceland, leads to precipitation of silver sulphide and quantitative loss of silver from solution*".

Observations in active geothermal systems also support the interpretation that boiling is an effective depositional mechanism for gold and silver. As an example, Brown (1986) examined silica scales that precipitate on the back-pressure plate in geothermal wells where the single-phase fluid undergoes boiling (flashing) as it passes through an orifice from the high pressure to low pressure side. The silica scale resulting from this process in well BR22 at Ohaaki, Broadlands, New Zealand, contained 2500 mg/kg Ag (2500 ppm) and 15 mg/kg (15 ppm) Au. Brown (1986) noted that "*the back-pressure plate provides an analogue of the processes that take place as the geothermal fluid rises through the earth's crust.*" and that "*Gold is deposited as fluid rises, due principally to the reduction in the amount of dissolved H_2S remaining in the liquid phase on boiling of the deep aquifer fluid*". Numerous studies of epithermal precious metals deposits have also concluded that boiling is the dominant depositional mechanism in many deposits. Among the first to recognize the genetic link between boiling and precious metal deposition were Kamilli and Ohmoto (1977) in the Finlandia, Peru deposit. These workers noted that "*The fine-grained nature of the Ag-Au-rich stage II ore, its strong control by elevation, and the observation that primary fluid inclusions exhibit markedly variable liquid to vapor volume ratios all indicate that boiling was the controlling factor in the ore formation for this stage.*" More recently, Simmons et al. (2005) compiled data from a large number of epithermal deposits, and 54 out of 83 deposits list boiling ± mixing as the depositional mechanism, with 11 of the studies not identifying a mechanism. Similarly, these same authors list among the critical genetic factors required for formation of epithermal deposits "*the development of boiling and/or mixing conditions which create sharp physical and chemical gradients conducive to precious and base metal precipitation*". Hedenquist et al. (2000) note that "*Boiling is the process that most favors precipitation of bisulfide-complexed metals such as gold*" and in discussing the importance of boiling in ore formation and in exploration state that "*Thus, evidence for boiling to have occurred in an epithermal environment is desirable because it can lead to deposition of high-grade gold ore*".

It should be noted that boiling is not the depositional mechanism in *all* epithermal deposits. As noted above, 18 out of 83 deposits compiled by Simmons et al. (2005) list a process other than boiling as the depositional mechanism – in most cases it is mixing and/or cooling. Similarly, Albinson et al. (2001) evaluated 52 low-sulfidation precious and base metal deposits in Mexico (including those in the Guanajuato district) and classify some deposits, such as Sombrerete, Zacatecas, as non-boiling systems based on the absence of vapor-rich inclusions, lack of platy or lattice calcite, lack of adularia and presence of predominantly coarsely crystalline varieties of quartz, i.e., lack of crustiform-colloform banded silica. Hedenquist et al. (2000) report that, while boiling may not have occurred during the precipitation of sulfides and gold in high sulfidation deposits and that boiling may not be the sole precipitation mechanism, "*Regardless, boiling must occur at some stage in the life of high-sulfidation systems, as indicated by the common occurrence of hydrothermal breccias, ….*". In such systems, evidence of boiling is considered to be a positive factor in exploration, even if boiling is not genetically associated with gold mineralization.

In this study, we assume that the dominant depositional mechanism associated with precious metal mineralization on the La Luz vein system at Guanajuato is boiling. This assertion is supported by earlier work of Buchanan (1980) on the adjacent Veta Madre in the Guanajuato district, as well as our own studies of other deposits along the Veta Madre (Moncada and Bodnar, 2012a,b,c; Moncada et al., 2012).

5.2. Evidence of boiling

Various mineralogical, textural and fluid inclusion features have been genetically linked with boiling in the epithermal environment. Coexisting liquid-rich and vapor-rich fluid inclusions contained *in the same Fluid Inclusion Assemblage* (FIA; Goldstein and Reynolds, 1994) (Fig. 3A) provide unarguable proof of the presence of boiling fluids (Bodnar et al., 1985). Similarly, if intense boiling or flashing occurs such that little or no liquid remains in the system, FIAs composed of only vapor-rich inclusions may result (Fig. 3B). Thus, according to Albinson et al. (2001), "*Fluid inclusion assemblages consisting solely of vapor-rich inclusions are also considered evidence that boiling occurred in the fluids*".

When boiling occurs, the phases that are precipitated may be amorphous or so fine-grained that trapping of fluid inclusions is not possible. However, the boiling fluids that are precipitating the amorphous/fine-grained phases may be trapped as secondary inclusions in earlier precipitated phases that have since crystallized (or re-crystallized) to produce coarser grained phases that are amenable to hosting fluid inclusions. Thus, secondary fluid inclusions become important tools for recognizing that boiling occurred, even though the boiling event that is being recorded by the inclusions occurred after the material hosting the inclusions was originally precipitated. These secondary inclusions trapped from boiling fluids also provide valuable information concerning the pressure (depth) of formation, which, in turn, can be used to estimate depth below the paleo-water table. In discussing fluid inclusions in such material, Sander and Black (1988) state "*We suggest that some such zones were originally deposited as metastable, hydrous chalcedony or amorphous silica. Fluid inclusions contained within them were created during postdepositional recrystallization of the original host to quartz.*"

Boiling also leads to distinct mineralogy and mineral textures in the epithermal environment owing to the physical and chemical changes that take place as a result of boiling, including rapid temperature decrease, decrease in the amount of liquid available to accommodate the dissolved components, and loss of gases that lead to changes in fluid chemistry. For example, consider a non-

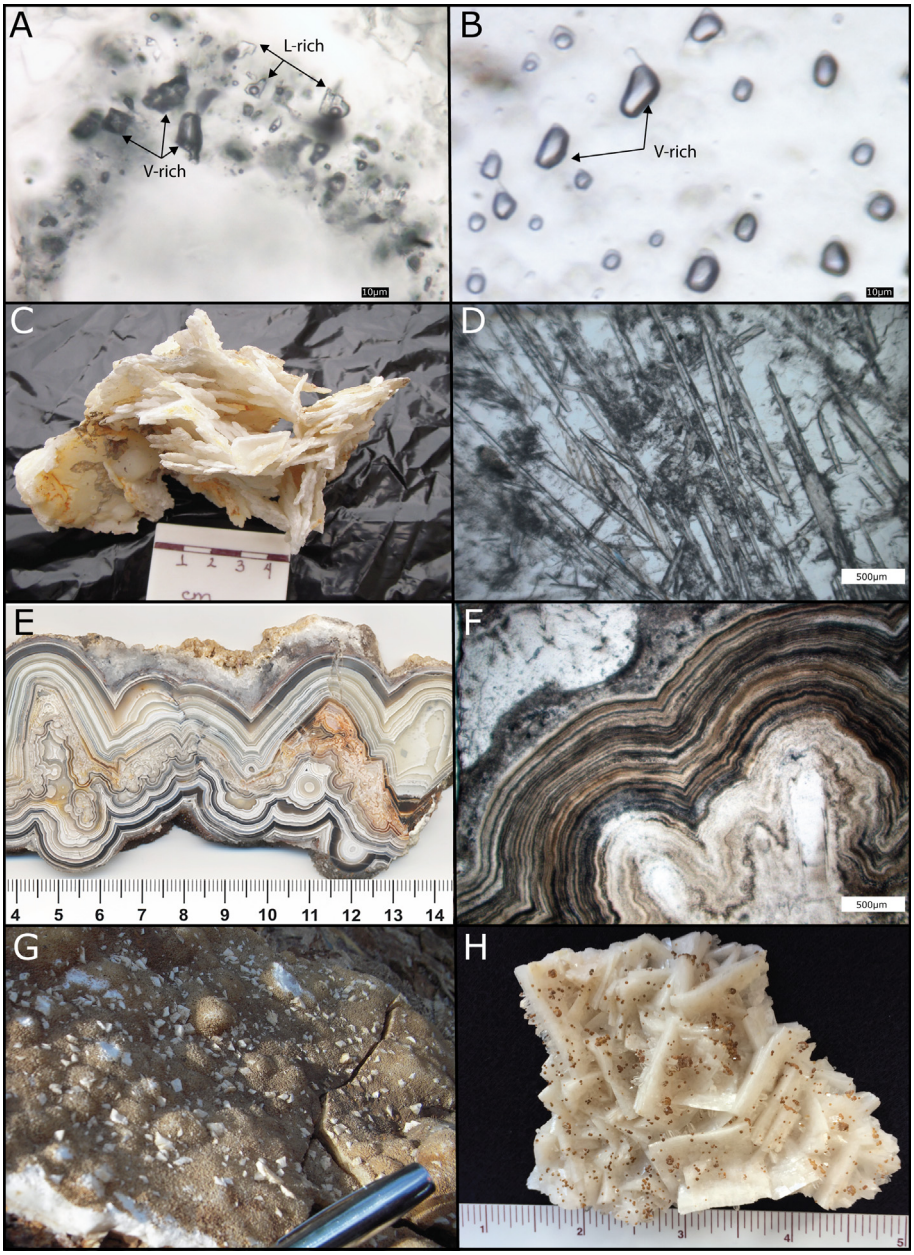

Fig. 3. Fluid inclusion, mineralogical and textural features associated with boiling fluids. A. Primary Fluid Inclusion Assemblage consisting of coexisting liquid-rich and vapor-rich inclusions in quartz. B. Secondary Fluid Inclusion Assemblage consisting of only vapor-rich inclusions in quartz. C. Hand sample of bladed (platy) calcite. D. Photomicrograph of bladed calcite replaced by quartz. E. Hand sample showing colloform quartz. F. Photomicrograph showing colloform quartz in thin section. G. Outcrop covered by numerous small (white) adularia crystals from the La Luz vein system. H. Hand sample of adularia from the La Valenciana historical mine in the Guanajuato district.

boiling hydrothermal fluid that enters the base of a hydrothermal system and begins to boil adiabatically as it flows upwards and remains on the liquid-vapor (boiling) curve. If 25% of the liquid is converted to vapor (steam) as a result of boiling, enthalpy (heat) balance requires that the temperature would decrease to 200 °C. In a typical shallow geothermal environment, this may happen over a vertical distance of a few hundred meters, representing a geothermal gradient of several hundred degrees Celsius per kilometer. The silica content of the hydrothermal fluid (liquid) entering the bottom of the ore zone at 300 °C would be 633 mg/kg as defined by quartz solubility in H_2O at these conditions (Gunnarsson and Arnórsson, 2000). The silica solubility at 200 °C is controlled by chalcedony solubility and would be 340 mg/kg (Gunnarsson and Arnórsson, 2000). However, 25% less liquid phase remains at 200 °C compared to the amount of liquid that entered the base of the system, resulting in deposition of a total of 379 mg of SiO_2 for every kg of quartz-saturated liquid that enters the base of the system. The significant decrease in temperature over a short vertical distance, combined with the large decrease in dissolved SiO_2 associated with the temperature decrease and the change in solubility control from quartz to chalcedony, leads to significant oversaturation in SiO_2 and precipitation of amorphous silica to produce a colloform, banded texture. The amorphous silica eventually crystallizes to quartz but retains the banded texture that is common in epithermal deposits (Fig. 3E).

Dong et al. (1995) describe various textures that record the presence of a silica gel precursor, including colloform (Fig. 3E, F), moss, ghost sphere, flamboyant and pseudoacicular textures. These

same workers conclude that "... *the presence of quartz textures inherited from silica gel, along with other geological, mineralogical, or fluid inclusion evidence of relatively high temperatures, is a good indicator of boiling in epithermal environments*". Some textures, such as mosaic (jigsaw), feathery, flamboyant, plumose and ghost sphere are thought to represent (re)-crystallization of amorphous silica or chalcedony (Dong et al., 1995) that may have precipitated from boiling solutions or as a result of some other process such as rapid cooling or fluid mixing. These textures are less diagnostic of boiling than the others listed above.

Calcite is a common mineral in epithermal deposits, and the crystal form and habit can be indicators of depositional conditions. In particular, Simmons and Christenson (1994) have shown that platy (or lattice/bladed) calcite (Fig. 3C, D) forms in the upflow zone of epithermal systems as a result of exsolution of CO_2 from the fluid as the fluid boils. The loss of CO_2 to the vapor results in the rapid precipitation of calcite, which favors formation of platy or bladed crystals rather than rhombohedral crystals that form during slower growth. Thus, the presence of platy/bladed calcite is strong evidence for boiling in the epithermal environment.

The loss of CO_2 to the vapor also results in an increase in the pH of the fluid, which leads to a shift from illite to adularia stability. At 250 °C, a fluid with a neutral pH, activity of O_2 of $\sim 10^{-37}$, activity of sulfur of 0.01, and containing 5×10^{-3} m K^+ and 4×10^{-5} m Mg^{++} that is precipitating (in equilibrium with) quartz would also be in equilibrium with illite (Fig. 4). If that same fluid starts to boil, the increase in pH of the fluid associated with boiling as CO_2 is lost to the vapor moves the fluid composition into the adularia stability field (i.e., to the right of the quartz/illite/adularia equilibrium line on Fig. 4). Similarly, if upon boiling the silica phase that is precipitating changes from quartz to amorphous silica, illite stability is shifted to much lower pH values (Fig. 4), and adularia becomes the stable phase in equilibrium with amorphous silica. Thus, adularia is an indicator of boiling conditions in the epithermal environment (Fig. 3G, H). We also infer from these phase equilibria relationships that a sample containing FIAs consisting of liquid-rich inclusions with trapped illite and other FIAs consisting of either coexisting liquid-rich and vapor-rich inclusions, or only vapor-rich inclusions, or both, in the same sample is evidence that fluids boiled episodically at that location. During nonboiling periods, fluids precipitating quartz and illite would be trapped (occasionally trapping an illite solid along with the liquid), whereas when boiling began and amorphous silica was the stable silica phase being precipitated, adularia would precipitate instead of illite, and earlier formed quartz would trap secondary FIAs consisting of coexisting liquid-rich and vapor-rich inclusions, or trails of vapor-rich only inclusions during flashing events.

In summary, the most diagnostic evidence for boiling in epithermal deposits is the presence of FIAs consisting of coexisting liquid-rich and vapor-rich fluid inclusions. FIAs composed of only vapor-rich inclusions suggest that boiling occurred, but boiling could have occurred at some considerable depth (higher pressure) below that corresponding to the current sample location. The presence of adularia, bladed/platy/lattice calcite or colloform banded quartz are all also considered to be strong evidence of boiling. Other quartz textures that suggest original precipitation of silica gel (amorphous silica) or chalcedony, such as jigsaw/mosaic, feathery, plumose, flamboyant and ghost sphere quartz are consistent with deposition from boiling solutions but could form from other processes that result in rapid silica precipitation. Thus, we include colloform quartz, adularia and bladed calcite as being the best mineralogical/textural evidence that boiling conditions prevailed, as also noted by Simmons and Browne (2000) who state that "... *the occurrence of platy calcite, crustiform-colloform silica, and K feldspar [adularia] in veins indicates the existence of boiling conditions conducive to precious-metal deposition*".

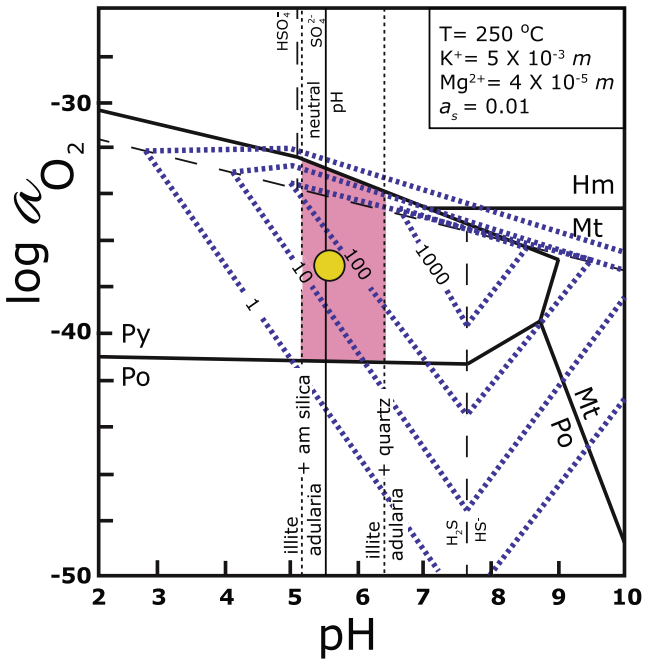

Fig. 4. Solubility of Au at 250 °C as a function of the activity of oxygen and pH, modified from Henley and Brown (1985) and Shenberger and Barnes (1989). Solubility contours (in ppb) are shown by dashed lines. The yellow dot represents a fluid of neutral pH in equilibrium with pyrite, quartz and illite. During boiling and loss of CO_2 to the vapor, the pH will increase (i.e., the yellow dot will move to the right) and quartz and pyrite would be in equilibrium with adularia rather than illite at pH values greater than about 6.4. Similarly, if the silica phase that precipitates when the fluid boils changes from quartz to amorphous silica, the fluid would be in equilibrium with adularia, even if the pH does not increase.

5.3. Spatial relationship between boiling and mineralization

Studies of many epithermal deposits, as well as observations in active continental geothermal systems, indicate that once boiling begins at depth the fluid continues to boil to the surface (or to the water table). Moreover, Hedenquist et al. (2000) and Simmons and Browne (2000) report that boiling most often occurs in the upflow zones where deep fluids migrate rapidly towards the surface. The upflow zones also represent the zones in which gangue and ore minerals are precipitated to form the silica-dominated veins that are characteristic of low to intermediate sulfidation precious metal deposits. Additionally, Albinson et al. (2001) note that, in systems in which boiling is the depositional mechanism, there is a sharp cutoff in grades at the bottom of the ore zone that corresponds approximately with the bottom of the boiling zones. Highest grades are typically found at various distances above the deepest levels at which boiling is observed, and the ore zone typically extends over a vertical distance of a few hundred meters. Even though boiling continues to the surface, metal grades might be very low in surface samples as all the metal was deposited at greater depths, deeper within the boiling zone. Thus, low metal grades do not preclude the possibility of significant mineralization at greater depth, if the samples show good evidence of boiling.

5.4. Boiling Confidence Factor

Assuming that precious metal precipitation is triggered by boiling as suggested by numerous and varied experimental studies and observations in active continental geothermal systems and their fossil equivalents, the epithermal deposits, it is desirable to have a scoring method to rate and prioritize samples or locations for fur-

ther evaluation during exploration for precious metal mineralization. Previously, Moncada et al. (2012) described a Boiling Intensity Factor that was meant to identify those samples showing the strongest evidence of boiling. Here, we describe the Boiling Confidence Factor that is intended to replace and improve upon the concept put forth by the Boiling Intensity Factor.

Our basic assumption is that one can be more confident that boiling occurred at a given location if the sample shows multiple features that are indicative of boiling rather than only one or two such features. Moreover, some features, such as the presence of FIAs containing coexisting liquid-rich and vapor-rich inclusions that were not produced by leakage or other reequilibration processes are unarguable proof of the former existence of liquid and vapor in the vein system. Other features, such as FIAs consisting of only vapor-rich inclusions, or adularia, colloform quartz or bladed calcite, strongly support an origin via boiling but these features could be produced by other mechanisms. Finally, quartz textures that suggest original precipitation of silica gel (amorphous silica) or chalcedony, such as jigsaw/mosaic, feathery, plumose, flamboyant and ghost sphere quartz are consistent with deposition from boiling solutions, but these textures could result from other processes that lead to rapid silica precipitation.

Based on how confident one can be that a given feature described above is the result of boiling, we assign the following Confidence Factors to these features. The presence of FIAs containing coexisting liquid-rich and vapor-rich inclusions is assigned a value of 5 (five) as it is conclusive evidence that liquid and vapor were present at some time and at the location where the sample was collected. Fluid Inclusion Assemblages consisting of vapor-rich inclusions only, the presence of bladed (or platy) calcite and/or bladed calcite replaced by quartz, colloform (banded) quartz and adularia are each assigned a numerical score of 3 (three). Quartz textures that suggest recrystallization of silica that was originally precipitated as silica gel (amorphous silica) and/or chalcedony, and which are less diagnostic of boiling conditions, such as jigsaw/mosaic, feathery, plumose, flamboyant and ghost sphere quartz are all assigned a value of 1. The total Boiling Confidence Factor (BCF) assigned to each sample represents the sum of all features present, multiplied by their individual confidence ratings. Thus, a sample with FIAs containing coexisting liquid-rich and vapor-rich inclusions (5), colloform quartz (3), adularia (3) and jigsaw quartz (1) would have a boiling confidence factor of 5 + 3 + 3 + 1 = 12. The maximum BCF that a sample may have according to this formulation is 20.

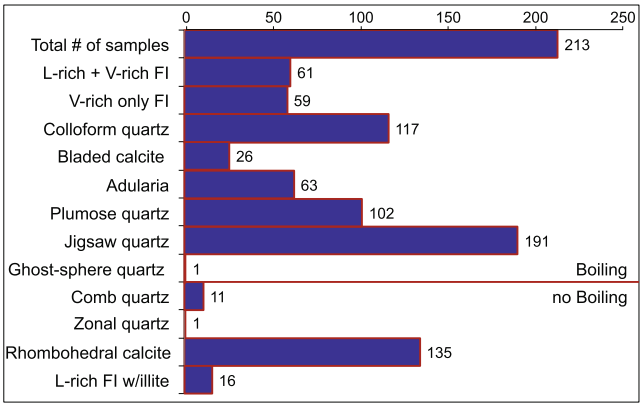

Fig. 5. Relative abundance of the different mineralogical, textural and fluid inclusion characteristics observed in samples from the La Luz area. The number at the end of each bar represents the number of samples (out of the total of 213 samples examined) that exhibit the feature listed. Liquid-rich + vapor-rich fluid inclusions, vapor-rich fluid inclusions only, colloform quartz, bladed calcite, adularia, plumose quartz, jigsaw quartz and ghost-sphere quartz are all features that are interpreted to be associated with boiling fluids, whereas comb and zonal quartz, rhombohedral calcite and liquid-rich fluid inclusions with illite are thought to form during nonboiling (or slow growth) conditions. Note that the sum of all the histograms is greater than the total number of samples because most samples exhibit more than one of the listed features.

We recognize that the means of quantifying the likelihood that boiling occurred described above is simplistic, but it is an approach that we have found to be effective in distinguishing between samples/locations where the probability that boiling occurred is high, and those locations where there is less confidence that boiling occurred. We also emphasize that the BCF is one of many tools that might be applied in an exploration program, and the BCF results are not intended to be used in lieu of, or in the absence of, other geologic, geochemical, geophysical and structural information that might be available.

Various features described above that are related to boiling conditions, as well as features that are considered to be evidence for non-boiling conditions, such as comb and zonal quartz, rhombohedral calcite and fluid inclusions with trapped illite, have been compiled for all 213 samples collected from the La Luz area. The number of samples showing each of the various features is summarized in Fig. 5.

6. Mineralogy and paragenesis

Veins in the La Luz area are characterized by textures indicating sequential precipitation in open fractures. The different events define a paragenetic sequence that can be divided into five stages (Fig. 2). Each stage is characterized by a specific assemblage of gangue and ore minerals, mineral textures and fluid inclusion types. The ore minerals include acanthite and the sulfosalts pyrargyrite and polybasite. Minor amounts of cinnabar, sphalerite and chalcopyrite also occur.

Gangue and ore minerals show a distinct evolution during the various stages of mineralization (Fig. 2). Stage I is characterized by rhombohedral calcite in horizontal veins, with zonal to comb quartz appearing near the end of this stage. Stage I includes the unmineralized 240° veins that are perpendicular to the main La Luz veins. Stage II is characterized by zonal and comb quartz followed by rhombohedral calcite with associated epidote alteration and jigsaw quartz appearing near the end of this stage. Stage III contains zonal and comb quartz with small amounts of pyrite and rhombohedral calcite. A breccia containing fragments of wallrock that have been cemented by jigsaw quartz and containing pyrite with traces of Au and Ag appears near the end of stage III. Plumose quartz, bladed calcite replaced by quartz, colloform quartz, and traces of acanthite also appear at the end of stage III. Stage IV hosts the ore and is characterized by argentiferous pyrite within jigsaw quartz and by acanthite and miargyrite disseminated within colloform quartz and associated with plumose quartz. Minor electrum is present near the end of stage IV and sulfosalts and adularia occur at the end of stage IV and beginning of stage V. Bladed calcite appears late in stage III and throughout stage IV and, in some samples, continues into early stage V. Rounded fragments with calcite and quartz cemented by jigsaw quartz are present in stage IV. Finally, in stage V, rhombohedral calcite, cinnabar, amethyst, zonal and comb quartz, jigsaw and ghost-sphere quartz are present (Fig. 2). Brecciation and repetition of textures and minerals characteristic of boiling suggests that several episodes of boiling occurred during the Ag and Au mineralization stage of the paragenetic sequence.

7. Data and results

Samples were collected from the main mineralized veins, which generally strike 315° to 360°, as well as from a few veins with a

strike of 240° and oriented perpendicular to the main veins. Samples were obtained from surface outcrops, underground historical workings, and drill core. A description of the textural (petrographic) and mineralogical data for each vein from west to east in the district is summarized below, followed by a summary of the fluid inclusion microthermometric data for each vein.

7.1. Textures and petrography

7.1.1. Plateros vein

Samples were collected from the Plateros vein in the western part of the La Luz area (Fig. 1), as well as further south along a vein that is interpreted to be the southern extension of the Plateros vein (Fig. 6). Samples could not be collected in the central region because the area is occupied by dwellings and farm fields in some places, and the vein does not crop out at the surface at other locations. Samples were also collected at the Chayita and Chuparosa historical mine sites (Figs. 1 and 6) that are interpreted to be on the Plateros vein. Evidence of boiling includes colloform quartz, bladed calcite or bladed calcite replaced by quartz, adularia, and FIAs with coexisting liquid-rich and vapor-rich fluid inclusions and FIAs containing only vapor-rich fluid inclusions (Table A1). Most samples collected from the Plateros vein show some evidence of boiling, and the overall Boiling Confidence Factor (BCF) for individual samples ranges from 0 to 13 (Table A1 and Fig. 6). Some samples from the Plateros vein that show evidence of boiling also show elevated gold grades – for example, one sample with a BCF of 12 contains 2.9 ppm Au and 439 ppm Ag (sample Oct_2011_1056563; Table A1; Fig. 6). Other samples with elevated BCF values show poor Au and Ag grades – for example, one sample with BCF of 10 (sample Oct_2011_1056561; Table A1) and one with BCF of 13 (sample 1005-181; Table A1) contain 0 ppm Au and 2 ppm Ag and 0.04 ppm Au and 5 ppm Ag, respectively. One sample from the Chayita underground workings (sample Oct_2011_1056577; Table A1) shows a BCF of 5 and contains 2.62 ppm Au and 89 ppm Ag, and a sample from the Chuparosa underground workings (sample Oct_2011_1056575; Table A1) shows a BCF of 7 and contains 5.01 ppm Au and 15 ppm Ag. Importantly, no samples from the Plateros vein that contain >1 ppm Au and >10 ppm Ag show a BCF of less than 5 (Fig. 6; Table A1). Stated differently, no sample that shows little to no evidence of boiling contains elevated Au and/or Ag grades.

7.1.2. Melladito vein

The next vein to the east of the Plateros vein is the Melladito vein (Fig. 1). This vein has good exposure on the surface, and was also sampled from drill core (drill holes DDH-1, DDH-4, DDH-9, DDH-14, DDH-17 and DDH-21) and from underground historical mines (Nopal, San Pablo, Sangria, La Bóveda, San José, San José de Abajo, and San Francisco de Asís), providing good three-dimensional sampling.

Textures indicating boiling include colloform quartz, bladed calcite or bladed calcite replaced by quartz, and adularia. Samples from the surface to the greatest depths explored on the vein contain FIAs with coexisting liquid-rich and vapor-rich fluid inclusions, as well as FIAs consisting of only vapor-rich fluid inclusions. Some of the deeper samples collected from 2225 to 2375 m depth contain liquid-rich fluid inclusions with trapped illite crystals suggesting that conditions episodically varied from boiling to non-boiling at these depths, as described above (Fig. 4). The Boiling Confidence Factor for samples from the Melladito vein varies from 0 to 16 (Fig. 7; Table A1). Eighteen out of 72 samples collected from the Melladito vein contain >1 ppm Au, and the BCF for these 18 samples ranges from 4 to 16 (Table A1), with an average of 8.6. Eleven samples from the Melladito vein contain >100 ppm Ag, and the BCF of the 11 samples ranges from 4 to 12 (Table A1), with an average of 7.8. All samples with >5 ppm Au have BCF of ≥7. No sample with BCF <4 contains either >1 ppm Au or >100 ppm Ag.

The longitudinal section of the Melladito vein (Fig. 7B) shows that evidence of boiling is erratically distributed along the vein, with some samples showing no evidence or only weak evidence of boiling. Samples with the highest BCF on the Melladito vein usually correlate with high gold grades, such as in drill cores and at the San Pablo, Sangria and La Boveda mines. Silver grades are also heterogeneously distributed along the vein, with higher grades

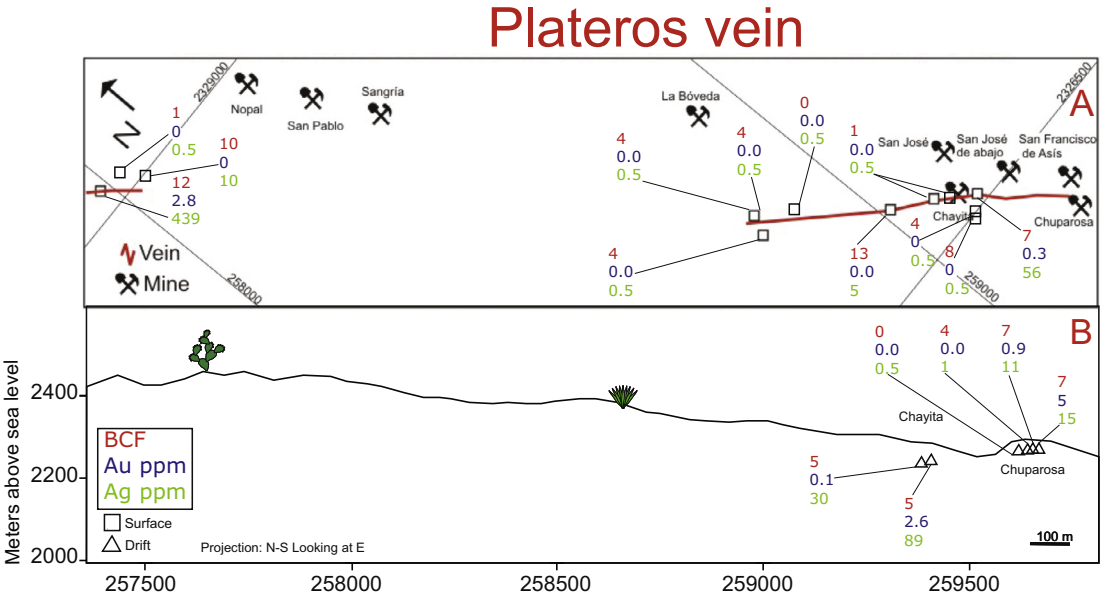

Fig. 6. (Top) Plan view of the Plateros vein at the San Ignacio property in the La Luz vein system at Guanajuato, Mexico showing surface sample locations. (Bottom) Longitudinal section showing location of underground samples from the Chayita and Chuparosa mines on the Plateros vein. The numbers linked to each sample location represent the Boiling Confidence Factor (BCF, red), Au grade in ppm (blue) and Ag grade in ppm (green). No vertical exaggeration. (For interpretation of the references to color in this figure legend, the reader is referred to the web version of this article.)

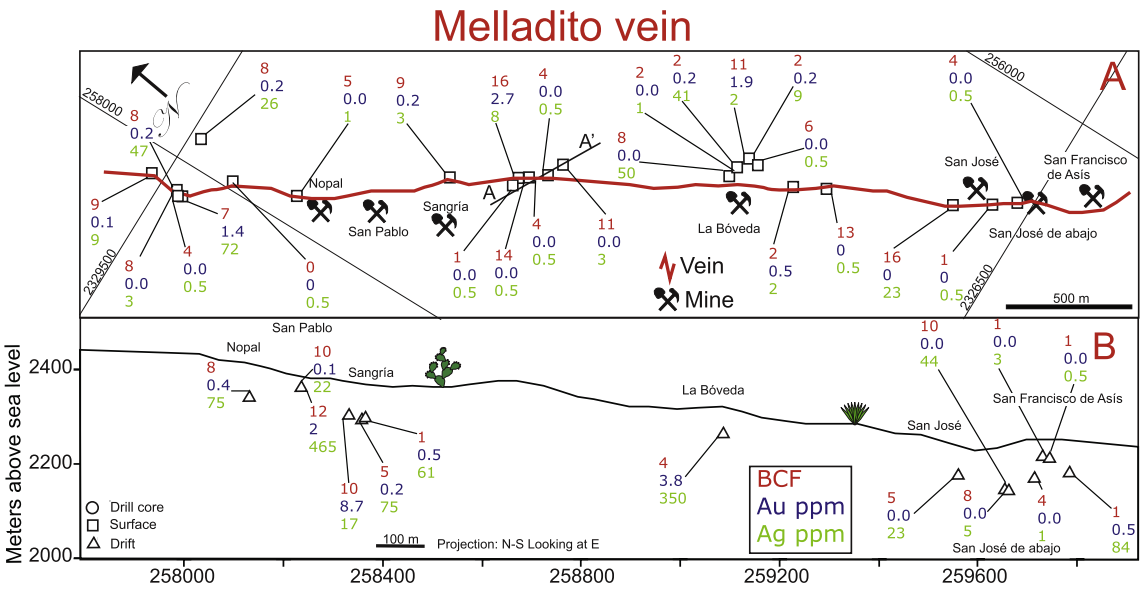

Fig. 7. (Top) Plan view of the Melladito vein in the La Luz vein system at Guanajuato, Mexico showing surface sample locations along the vein as well as perpendicular to the vein along traverse A – A′. (Bottom) Longitudinal section of the Melladito vein showing underground sampling locations. The numbers linked to each sample location represent the Boiling Confidence Factor (BCF, red), Au grade in ppm (blue) and Ag grade in ppm (green). No vertical exaggeration. (For interpretation of the references to color in this figure legend, the reader is referred to the web version of this article.)

(>50 ppm) in drill holes, and at the Nopal, San Pablo, Sangria, La Boveda and San Francisco de Asis mines.

7.1.3. Intermediate vein

The Intermediate vein does not outcrop at the surface and five samples were collected from drill holes. All samples show evidence of boiling, including FIAs containing coexisting liquid-rich and vapor-rich fluid inclusions and FIAs containing only vapor-rich fluid inclusions. Gangue minerals and textures indicating boiling include colloform quartz, plumose quartz, jigsaw quartz and adularia. The boiling confidence factor ranges from 4 to 10 (Table A1; Fig. 8).

The sample (1305-264; Table A1) with both the highest Au grade (2.34 ppm) and the highest Ag grade (709 ppm) has a BCF of 8 (Fig. 8). The sample from the Intermediate vein with the highest BCF of 10 (sample 1305–270; Table A1; Fig 8) contains 0.81 ppm Au and 83 ppm Ag.

7.1.4. Nombre de Dios vein

The Nombre de Dios vein is located in the west-central part of the La Luz area (Fig. 1). Fifteen samples were collected from surface outcrops and drill holes. Most samples show moderate to strong evidence of boiling, including coexisting liquid-rich and vapor-rich fluid inclusions and FIAs consisting of only vapor-rich fluid inclusions. Gangue minerals and textures providing evidence of boiling include colloform quartz, plumose quartz, jigsaw quartz, bladed calcite or bladed calcite replaced by quartz, and adularia. The boiling confidence factor ranges from 1 to 16, with thirteen of the samples having BCF ≥5, and six of the samples having BCF ≥10 (Fig. 9; Table A1). The highest Au grades (2.02, 3.03 and 8.26 ppm) are from samples with BCF of 13, 16 and 13, respectively

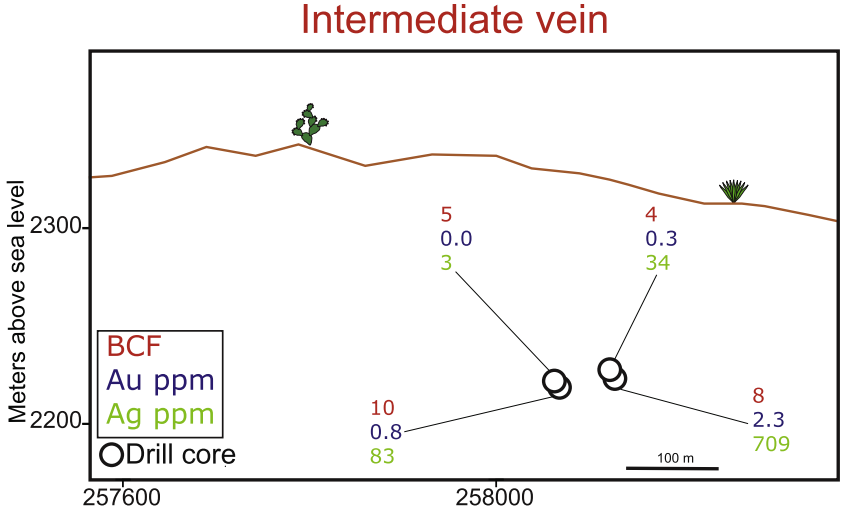

Fig. 8. Longitudinal section of the Intermediate vein in the La Luz vein system at Guanajuato, Mexico showing sample locations. The numbers linked to each sample location represent the Boiling Confidence Factor (BCF, red), Au grade in ppm (blue) and Ag grade in ppm (green). No vertical exaggeration. (For interpretation of the references to color in this figure legend, the reader is referred to the web version of this article.)

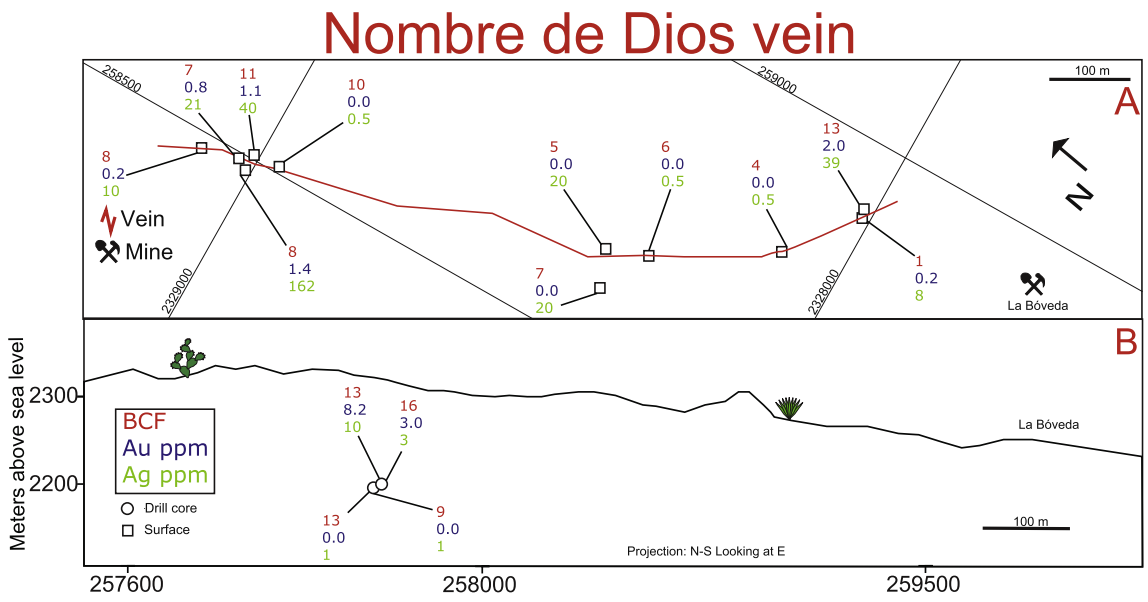

Fig. 9. (Top) Plan view of the Nombre de Dios vein in the La Luz area showing surface sample locations. (Bottom) Longitudinal section of the Nombre de Dios vein showing drill core sample locations. The numbers linked to each sample location represent the Boiling Confidence Factor (BCF, red), Au grade in ppm (blue) and Ag grade in ppm (green). No vertical exaggeration. (For interpretation of the references to color in this figure legend, the reader is referred to the web version of this article.)

(Fig. 9; Table A1). The sample with the highest Ag grades (162 ppm, sample 305-04; Table A1; Fig. 9) has a BCF of 8 and, in general, there is little correlation between Ag grades and BCF. For example, the sample with the highest BCF of 16 contains only 3 ppm Ag.

The longitudinal section of the Nombre de Dios vein (Fig. 9, bottom) shows the Boiling Confidence Factor for two samples where the Nombre de Dios vein was intersected by drill holes. Both samples show strong evidence of boiling, although both have low Ag values. The sample with a BCF of 13 has 8.2 ppm Au.

7.1.5. Bolañitos vein

Ten samples were collected from the Bolañitos vein in the underground workings of the active Bolañitos mine that is located in the northern part of the La Luz area (Fig. 1). A longitudinal section of the Bolañitos vein (Fig. 10) shows locations of samples from level 29606 and from approximately 50 m below this level. Most samples collected from this vein contain good evidence of boiling, including FIAs with coexisting liquid-rich and vapor-rich fluid inclusions, FIAs with only vapor-rich inclusions, colloform quartz, plumose quartz, jigsaw quartz and adularia.

The boiling confidence factor for the ten samples ranges from 1 to 16, with 8 of the 10 samples having BCF ≥7 (Table A1; Fig. 10). Gold grades show poor correlation with BCF, with one sample with BCF = 16 containing only 0.7 ppm Au, while another sample with BCF = 7 contains 2.5 ppm Au (Table A1; Fig. 10). Silver grades are high in all samples, as is expected for samples collected along

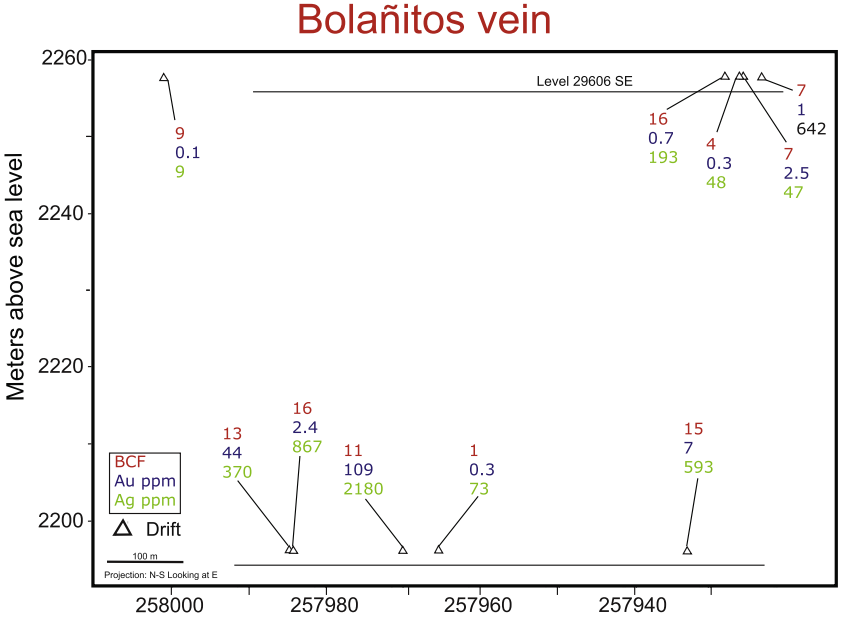

Fig. 10. Longitudinal section of the Bolañitos vein (along a N-S projection and looking east) in the La Luz vein system at Guanajuato, Mexico, with underground sample locations. The numbers linked to each sample location represent the Boiling Confidence Factor (BCF, red), Au grade in ppm (blue) and Ag grade in ppm (green). No vertical exaggeration. (For interpretation of the references to color in this figure legend, the reader is referred to the web version of this article.)

active mining faces from an operating silver mine. Silver grades range from 9 to 2180 ppm, with six of the samples containing ≥193 ppm (Table A1; Fig. 10). The highest Au grade (109 ppm) and the highest Ag grade (2180 ppm) are from the same sample (Sample 1401-39; Table A1) that has a BCF of 11 (Fig. 10).

The Boiling Confidence Factor for samples from the Bolañitos mine show very strong evidence of boiling in three of the four samples from the lower drift, suggesting that the bottom of the boiling zone, and the bottom of the mineralized zone, is at greater depths.

7.1.6. San José vein

Only one sample was collected underground from the San José vein (Fig. 1) which returned 5.2 ppm Au and 3430 ppm Ag (Table A1). The sample contains FIAs consisting of only vapor-rich inclusions (indicating intense boiling or flashing), jigsaw quartz and adularia. The BCF for this sample is 7 (Table A1).

7.1.7. Lucero vein

Samples from the Lucero vein were collected from drill holes and from underground workings in the Lucero extension of the Bolañitos mine. Most samples show moderate to strong evidence of boiling, including FIAs with only vapor-rich inclusions and FIAs with coexisting liquid-rich and vapor-rich inclusions, and colloform, plumose, and jigsaw quartz, and adularia. In the deepest levels, one sample contains liquid-rich inclusions with trapped illite, a feature that we interpret to be associated with the transition from non-boiling to boiling conditions based on phase equilibrium constraints (Fig. 4).

The BCF of samples from the Lucero vein varies from 1 to 16, with 9 of the 20 samples having BCF ≥ 10 (Fig. 11; Table A1). The sample with the highest silver grade (6780 ppm) and the highest gold grade (22.8 ppm) was collected from the underground workings (sample 1401-43; Table A1) and has a BCF of 10. The sample with the second-highest Ag grade (1120 ppm) is also from the underground workings and also has BCF = 10. Seven of the eight samples containing >150 ppm Ag have BCF ≥ 8 (with 6 having BCF ≥ 10), with one sample having BCF = 4. Nine of eleven samples containing >1 ppm Au have BCF ≥ 7, although one sample with BCF = 11 contains only 0.7 ppm Au and one with BCF = 10 does not contain detectable gold (Table A1).

The Boiling Confidence Factor of samples from underground workings and drill cores on the Lucero vein show evidence for boiling in the deepest samples collected (Fig. 11), indicating that the bottom of the boiling horizon is below the deepest levels explored.

7.1.8. Karina vein

Eight samples were collected on the Karina vein from drill holes, from one surface outcrop, and from underground workings along an extension to the south of the Bolañitos mine. All samples show moderate to strong evidence of boiling, including coexisting liquid-rich and vapor-rich inclusions, FIAs with only vapor-rich inclusions, colloform quartz, plumose quartz, jigsaw quartz and adularia (Table A1; Fig. 12). The longitudinal section of the Karina vein (Fig. 12) shows the Boiling Confidence Factor for samples from

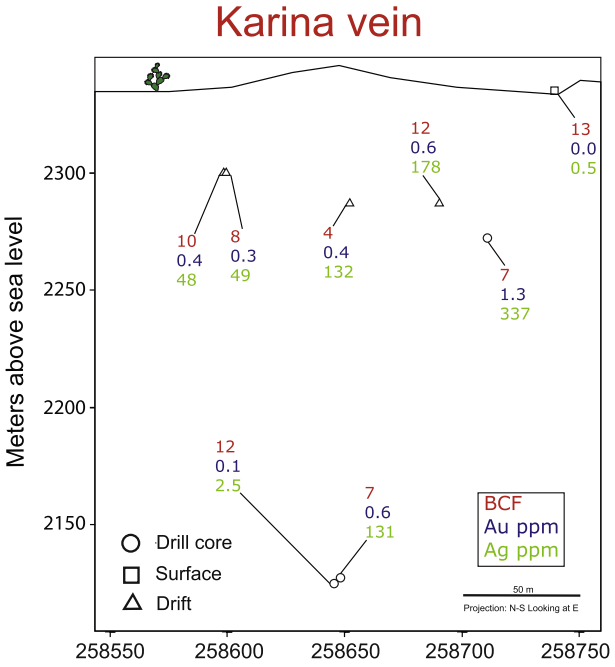

Fig. 12. Longitudinal section of the Karina vein in the La Luz vein system at Guanajuato, Mexico showing surface, drill core, and underground sampling locations. The numbers linked to each sample location represent the Boiling Confidence Factor (BCF, red), Au grade in ppm (blue) and Ag grade in ppm (green). No vertical exaggeration. (For interpretation of the references to color in this figure legend, the reader is referred to the web version of this article.)

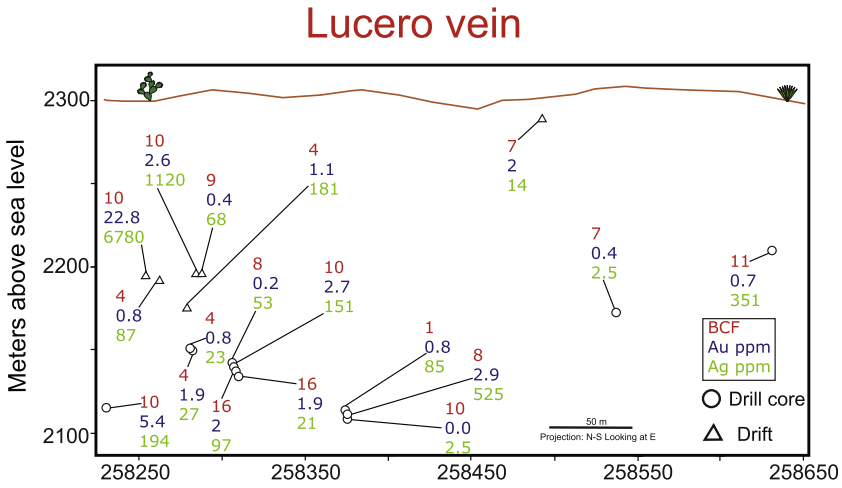

Fig. 11. Longitudinal section of the Lucero vein in the La Luz vein system at Guanajuato, Mexico, along a N-S projection and looking east. Open circles correspond to drill core samples, and open triangles correspond to drift samples. The numbers linked to each sample location represent the Boiling Confidence Factor (BCF, red), Au grade in ppm (blue) and Ag grade in ppm (green). No vertical exaggeration.(For interpretation of the references to color in this figure legend, the reader is referred to the web version of this article.)

underground workings and drill cores. The boiling confidence factor varies from 4 to 13, with seven of the eight samples showing BCF ≥ 7. Only one sample contains >1 ppm Au, and this sample has BCF = 7. Four of the eight samples contain >130 ppm Ag, and the BCF of the four samples are 4, 7, 7 and 12. The sample with the highest BCF (=13) is represented by a surface sample that contains no detectable Au and only 0.5 ppm Ag, and one of two samples with the second highest BCF (=12) contains only 0.1 ppm Au and 2.5 ppm Ag. We interpret these low metal grades in samples with high BCF values to indicate that boiling was initiated at some depth beneath the current sample depth and that Au and Ag were precipitated closer to the bottom of the boiling horizon. This interpretation is supported by the fact that samples from greater depth obtained from drill core and underground workings show higher Au and Ag values (Table A1; Fig. 12).

7.1.9. Daniela vein

Thirteen samples were collected from surface outcrops, underground workings and drill core on the Daniela vein. The various features that are evidence of boiling show a systematic distribution with depth on the Karina vein. From the surface to 2250 MASL, FIAs with coexisting liquid-rich and vapor-rich fluid inclusions, FIAs with only vapor-rich fluid inclusions, colloform quartz, plumose quartz, jigsaw quartz, bladed calcite replaced by quartz and adularia were observed (Table A1). At 2200 MASL all of the above-mentioned features were present with the exception of bladed calcite replaced by quartz. The deepest samples contain only colloform quartz, plumose quartz, and jigsaw quartz.

The longitudinal section of the Daniela vein (Fig. 13) shows the Boiling Confidence Factor and Au and Ag grades of samples from the vein. The BCF for samples from the Karina vein are all ≥4, and eleven of the thirteen samples show BCF ≥ 7. Eight of the thirteen samples contain >1 ppm Au (including one with 33.7 ppm Au and one with 21.1 ppm Au), and the BCF of these samples are all ≥7. Seven samples contain >100 ppm Ag, and all show BCF ≥ 4. As with the Lucero vein described above, some samples with high BCF show low precious metal values. One sample with the maximum possible BCF (=16) shows undetectable Au and only 8 ppm Ag. As with similar samples from the Lucero vein, the sample with high BCF and low metal grades is from the surface, and this is interpreted to indicate that metals were precipitated at greater depth where the fluid began to boil as it migrated along upflow zones to the surface.

7.1.10. Belén vein

Only two samples were collected from the Belén vein – one from a surface outcrop and one from an adit on the vein, and they contain an average of 1 ppm Au and 123 ppm Ag (Table A1). The samples show evidence for boiling in the form of coexisting liquid-rich and vapor-rich inclusions, colloform quartz, jigsaw quartz and adularia.

7.1.11. Veins intersected in drill holes

The Melladito vein was intersected by drill holes DDH-9 and DDH-14 at essentially the same depth (within one meter). One sample from DDH-9 contains 2.96 ppm Au and 35 ppm Ag, whereas the sample from DDH-14 contains 0.18 ppm Au and 35 ppm Ag. The sample from DDH-9 contains adularia and has a BCF of 7, whereas the one from DDH-14 has a BCF of 4, the difference being that the DDH-9 sample contains adularia and that from DDH-14 does not – both samples exhibit colloform and jigsaw quartz (Table A1). No useful fluid inclusions were observed in either sample.

As with the Melladito vein, the Intermediate vein was intersected by drill holes DDH-9 and DDH-14 at similar depths (±1 m). Two samples of the vein were collected from each core, one where the core first intersected the vein from above and the second approximately 50 cm below, where the core passed out of the vein and into the wallrock. In both drill holes, the metal grades in the upper sample are lower (0.02 ppm Au and 3 ppm Ag in DDH-14 and 0.34 ppm Au and 34 ppm Ag in DDH-9) than those in the lower sample (81 ppm Au and 83 ppm Ag in DDH-14 and 2.34 ppm Au and 709 ppm Ag in DDH-9), although the significance of this observation, if any, is unclear. One interpretation is that the veins are not symmetrical with respect to distribution of mineralization, as is typical in veins that are exposed during mining. Evidence of boiling was present in all samples (Table A1).

The Nombre de Dios vein was also intersected by drill holes DDH-9 and DDH-14 at depths less than one meter apart. Samples from the upper part of the vein (where DDH-14 first intersects the vein) contain 0.01 ppm Au and 1 ppm Ag, whereas samples from the lower part just before the drill core exist the vein and enters wallrock show Au below detection limits and ~1 ppm Ag. Samples collected from the upper part of DDH-9 contain 8.26 ppm Au and 10 ppm Ag, whereas samples from the lower part contain 3.03 ppm Au and 3 ppm Ag. These results document the heterogeneous distribution of metal grades within the vein. Evidence of boiling is present in all samples (Table A1).

The results above document large variations in metal grades over small distances, even within the same vein. Also, in one vein (Intermediate) the lower part of the vein has higher grades, whereas in another vein (Nombre de Dios) the upper part has higher grades. All samples from both veins show evidence of boiling. Thus, while metal grades vary randomly and erratically, all

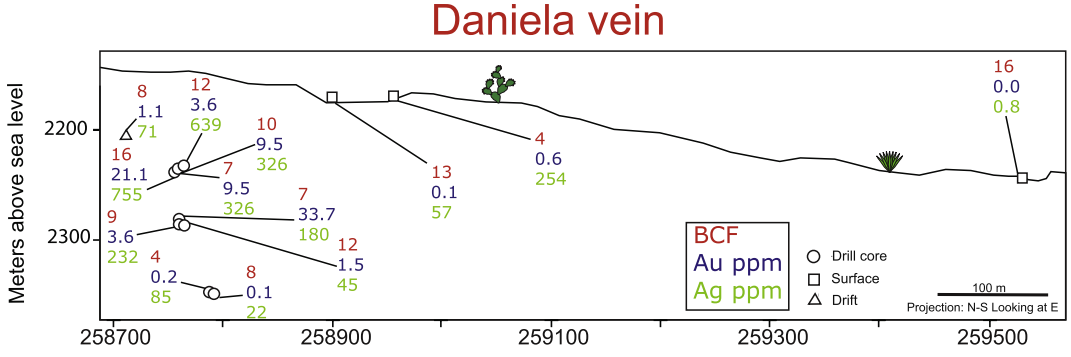

Fig. 13. Longitudinal section of the Daniela vein in the La Luz vein system at Guanajuato, Mexico with sample locations, plotted along a N-S projection looking east. Open circles correspond to drill core, open squares correspond to surface outcrops and open triangles correspond to drift samples. The numbers linked to each sample location represent the Boiling Confidence Factor (BCF, red), Au grade in ppm (blue) and Ag grade in ppm (green). No vertical exaggeration. (For interpretation of the references to color in this figure legend, the reader is referred to the web version of this article.)

samples show good evidence of boiling and indicate that further exploration in the area is warranted.

7.1.12. Section 28600

The Karina vein was intersected at two different depths in two different drill holes, and the Daniela vein was intersected at three different depths in three separate drill holes. The intersections are shown in section 28600 in Fig. 14. The Karina vein shows evidence of boiling (BCF = 7) where it is intersected at shallow depths by drill hole KA-15, and still shows evidence for boiling (BCF = 12) where it is intersected deeper by drill hole DN-1 (Fig. 14). The Daniela vein shows evidence of boiling based on fluid inclusions and mineral textures at three depths where it is intersected by drill holes DN-1 (shallow; BCF = 12), KA-15 (intermediate depth; BCF = 13) and DN-2 (deepest; BCF = 8) (Fig. 14). These results indicate that none of the drill holes intersected the veins at a depth that is beneath the deepest levels at which boiling occurred. Assuming that boiling and mineralization are related, these results suggest that additional precious metal resources might be discovered at greater depths on these veins.

7.1.13. Summary of textural and petrographic observations

The various textural and petrographic observations for veins in the La Luz area at Guanajuato, Mexico, are summarized in Fig. 15, which shows the complete depth range sampled for each vein and the depth range over which each of the various features was observed. All veins sampled show moderate to strong evidence of boiling in the deepest levels sampled.

7.2. Microthermometry

Only a few previous studies of fluid inclusions from the La Luz area have been reported (Mango, 1992; Vasallo and Reyes-Salas, 2007). Mango (1992) studied one sample from level 42 and another from level 32 (meters below current surface) on the Bolañitos vein. Homogenization temperatures of FI in calcite from level 42 ranged from 148 to 196 °C and salinity ranged from 0.7 to 1 wt.% NaCl. The sample of quartz from level 32 had a homogenization temperature of 206 °C and salinity of 0.2 wt.% NaCl. Vasallo and Reyes-Salas (2007) reported homogenization temperatures ranging from 230 to 253 °C for fluid inclusions in quartz associated with polybasite $(Ag,Cu)_{16}Sb_2S_{11}$. These previous studies did not report fluid inclusion evidence of boiling.

In this study, data were collected only from well-defined Fluid Inclusion Assemblages (FIAs) (Goldstein and Reynolds, 1994), representing groups of fluid inclusions that were trapped at the same time. Most FIAs studied here represent secondary fluid inclusions occurring along well-developed and clearly definable trails (healed microfractures; Fig. 3B). Fewer FIAs composed of primary inclusions (occurring along growth zones; Fig. 3A) were analyzed. FIAs in samples from the La Luz system were classified as containing (1) only liquid-rich inclusions with consistent liquid-to-vapor

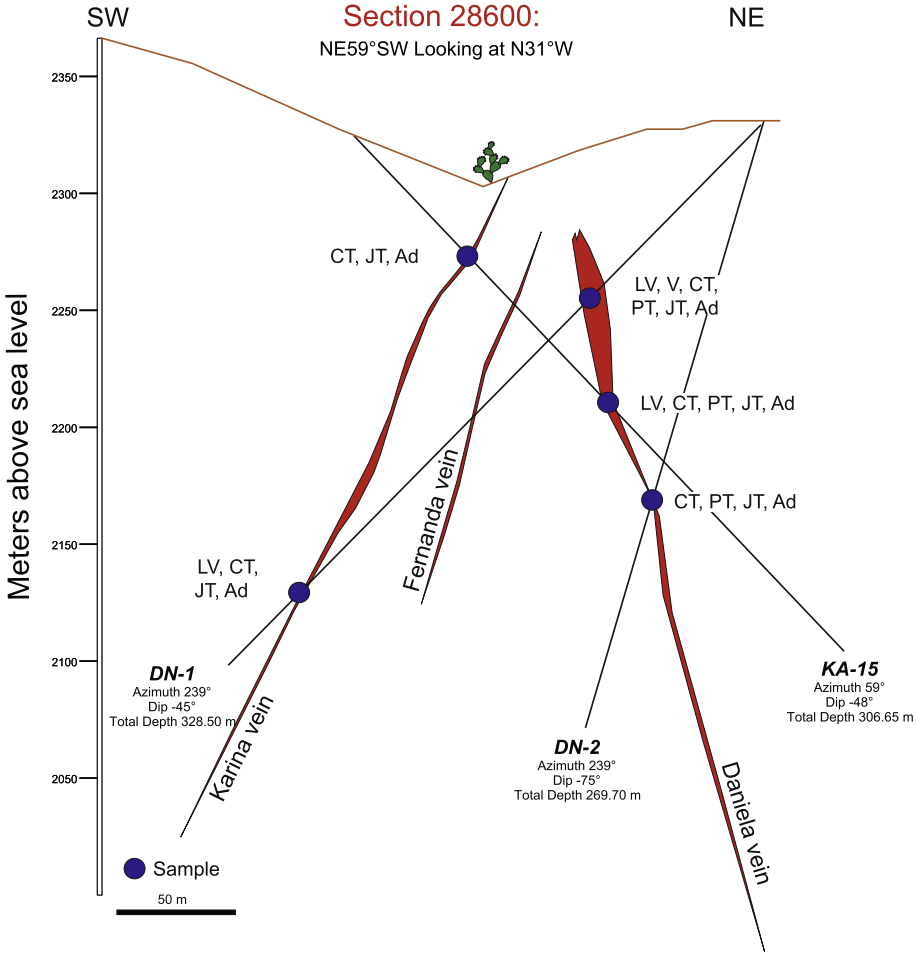

Fig. 14. Section 28600 showing the Karina and Daniela veins intersected at different depths by drill holes DN-1, DN-2, and KA-15. At each intersection, the boiling indicators that were observed are listed: LV = liquid-rich + vapor-rich fluid inclusions; V = only vapor-rich inclusions; CT = colloform quartz; PT = plumose quartz; JT = jigsaw quartz; BC = bladed calcite replaced by quartz; Ad = adularia.

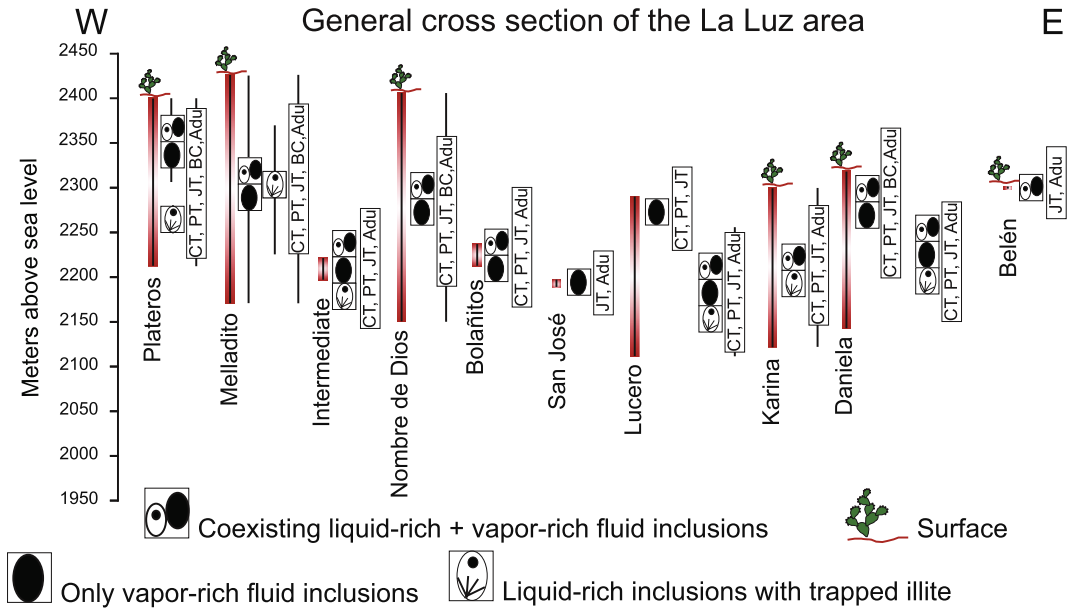

Fig. 15. Generalized cross section of the La Luz area showing the vertical distance over which various veins were sampled, and the vertical distribution over which various boiling indicators are observed. Veins with a cactus at the top outcrop at the surface, whereas those without a cactus do not outcrop.

ratios, (2) liquid-rich inclusions with consistent liquid-to-vapor ratios and containing a trapped illite crystal, (3) coexisting liquid-rich and vapor-rich inclusions with a broad range in liquid-to-vapor ratios, and (4) assemblages consisting of only vapor-rich inclusions.

Following detailed petrographic examination of the samples, 141 FIAs (representing 643 total fluid inclusions) were selected for microthermometric analysis. Inclusions were measured using a Linkam THMSG 600 heating/cooling stage mounted on a standard petrographic microscope. The stage was calibrated using synthetic fluid inclusion standards (Sterner and Bodnar, 1984). The precision and accuracy of measured homogenization temperatures are estimated to be ±1.0 °C and the precision and accuracy of ice-melting temperatures are estimated to be ±0.1 °C. The ice-melting temperatures were measured in order to estimate a fluid salinity to calculate boiling point with depth curves, but are not discussed further below. Note also that for FIAs consisting of coexisting liquid-rich and vapor-rich fluid inclusions, all reported ice-melting temperatures are for the liquid-rich inclusions in the assemblage.

The measured fluid inclusions are hosted by jigsaw quartz, plumose quartz, and bladed calcite and rhombohedral calcite as secondary fluid inclusion assemblages; primary fluid inclusions are present in euhedral quartz and in rhombohedral calcite. The homogenization temperatures of fluid inclusions from the La Luz system are described for each individual vein, from the west to the east including the Plateros, Melladito, Intermediate, Nombre de Dios, Bolañitos, San José, Lucero, Karina, Daniela and Belén veins. Microthermometric data for all FIAs studied are listed in Table 1 and summarized in Fig. 16 according to paragenetic stage.

Studies of epithermal Au-Ag deposits from around the world show that a majority of economic deposits formed at temperatures of less than about 300 °C, although some form at slightly higher temperatures. Thus, White and Hedenquist (1995) report that "*... epithermal ores form over the temperature range of <150 °C to ~300 °C ...*". Similarly, Simmons et al. (2005) report that "*Epithermal deposits are important sources of gold and silver that form at <1.5-km depth and <300 °C*". In describing Mexican epithermal deposits, Albinson et al. (2001) note that "*In deep-formed deposits, boiling occurs at temperatures that may exceed 300 °C*", but deposits on the Veta Madre (the vein system that parallels the La Luz vein system in the Guanajuato district) are not included among the deep deposits by Albinson et al. (2001) – these deposits are included in the shallow boiling deposit group.

Recognizing that fluids in some deep epithermal systems boil at temperatures >300 °C, we nevertheless here assume a maximum boiling temperature of 300 °C for fluids associated with mineralization on the La Luz vein system, consistent with our work as well as that of others in the district (Buchanan, 1979, 1980; Mango, 1992; Vasallo and Reyes-Salas, 2007). As such, it is desirable, from the exploration perspective to predict the depth to the 300 °C isotherm beneath the present surface or beneath the deepest levels explored through drill holes or underground workings. Studies of numerous epithermal deposits as well as their modern analogs, the continental geothermal systems, have shown quite clearly that once boiling begins at depth the fluid P-T conditions remain on the boiling curve as the fluid flows to the surface or the water table (c. f., Albinson et al., 2001, their Fig. 6; Vikre, 1985, his Fig. 15). Because the homogenization temperature of fluid inclusions trapped in a boiling system equals the formation or trapping temperature, the depth of the 300 °C isotherm may be calculated from the boiling point versus depth relationship (Haas, 1971). Thus, the homogenization temperatures of liquid-rich inclusions in all FIAs composed of coexisting liquid-rich and vapor-rich inclusions were measured to determine the temperature of boiling at the depth where the sample was collected (Fig. 17). Then, the depth to the 300 °C isotherm was calculated for each sample assuming that PT conditions remain on the boiling curve with increasing depth from that at which the sample was collected.

We emphasize that our goal in studying the fluid inclusions is only to determine if boiling occurred at the location where the sample was collected and, if so, the temperature at which boiling occurred. As noted above, much of the quartz in the veins was originally precipitated as amorphous silica and/or chalcedony and contains no fluid inclusions representative of the original depositional conditions. However, the quartz does contain abundant secondary fluid inclusions that represent the fluid that was present during some later stage in the overall history of the vein formation. If these secondary fluid inclusions show evidence of boiling, we assume that boiling occurred in that location at some time during

Table 1
Microthermometric data for fluid inclusions from the La Luz vein system sorted according to paragenetic stage. Fluid Inclusion Assemblages (FIA) consisting of coexisting liquid-rich and vapor rich fluid inclusions are highlighted in yellow, and the depth of trapping on the boiling curve corresponding to the average homogenization temperature of the FIA, as well as depth at which the fluid would be on the boiling curve at 300 °C, are also listed for these FIAs.

Paragenetic Stage	Sample no.	Vein	Host	FIA #	n	FI origin (P or S)	FI type	Th range (°C)	Average Th (°C)	Tm range (°C)	Average Tm (°C)	Salinity range (wt.% NaCl)	Average Salinity (wt.%)	Depth of trapping beneath paleosurface based on average Th and salinity	Depth of sample collection (m)	Depth to 300°C Isotherm
I	DM4	M	Qtz	1	4	S	L-rich	270-279	274	0 to -0.1	-0.1	0 to 0.2	0.1		-	-
I	905-180	Per	Qtz	2	6	S	L-rich	220-231	225	-0.5 to -0.7	-0.6	0.9 to 1.2	1.1		-	-
I	705-67	Per	Ca	1	2	P	L-rich	288-288	288	-0.4 to -0.5	-0.5	0.7 to 0.9	0.8		-	-
I	705-67	Per	Qtz	2	2	S	L-rich	262-280	271	-0.1 to -0.2	-0.2	0.2 to 0.4	0.3		-	-
I	905-180	Per	Qtz	1	4	S	L-rich	275-278	276	-0.2 to -0.3	-0.3	0.4 to 0.5	0.4		-	-
I	705-67	Per	Qtz	1	5	S	L-rich	193-199	196	-1.1 to -1.3	-1.2	1.9 to 2.2	2.1		-	-
I	705-67	Per	Qtz	1	7	S	L-rich	247-254	251	-0.5 to -0.7	-0.6	0.9 to 1.2	1		-	-
I	705-67	Per	Qtz	2	2	P	L-rich	236-237	236	-0.2 to -0.3	-0.3	0.4 to 0.5	0.4		-	-
I	705-63	Per	Qtz	1	2	S	L-rich	270-289	279	0 to -0.1	-0.1	0 to 0.2	0.1		-	-
I	705-63	Per	Qtz	1	3	S	L-rich	239-241	240	-0.1 to -0.2	-0.2	0.2 to 0.4	0.3		-	-
I	705-63	Per	Qtz	2	5	S	L-rich	198-213	206	-0.5 to -0.6	-0.5	0.9 to 1.1	0.9		-	-
I	305-07	Per	Qtz	1	2	S	L-rich	285-289	287	-0.3 to -0.4	-0.4	0.5 to 0.7	0.6		-	-
II	Oct_2011_1056563	P	Qtz	1	8	S	L-rich	187-209	198	-0.6 to -1	-0.7	1.1 to 1.7	1.3		-	-
II	564	M	Qtz	1	4	S	L-rich	200-225	215	-0.4 to -0.5	-0.4	0.7 to 0.9	0.7		-	-
II	564	M	Qtz	2	3	S	L-rich	213-218	215	-0.1 to -0.2	-0.1	0.2 to 0.4	0.2		-	-
II	564	M	Qtz	4	4	P	L-rich	199-199	199	-0.3 to -0.3	-0.3	0.5 to 0.5	0.5		-	-
II	705-70	M	Qtz	3	9	S	L-rich	198-223	212	-0.7 to -1	-0.9	0 to 1.7	1.3		-	-
II	1105-211	TM	Ca	1	6	S	L-rich	189-200	193	-0.8 to -1.3	-1	1.4 to 2.2	1.7		-	-
II	1105-202	TM	Qtz	1	4	P	L-rich	178-182	180	-0.2 to -0.6	-0.4	0.4 to 1.1	0.7		-	-
II	1105-202	TM	Qtz	1	6	S	L-rich	178-182	180	-0.5 to -0.6	-0.6	0.9 to 1.1	1		-	-
II	1105-202	TM	Ca	2	4	P	L-rich	180-185	183	-0.5 to -0.6	-0.6	0.9 to 1.1	1		-	-
II	1405-270	I	Ca	1	6	S	L-rich	158-160	159	-0.4 to -0.5	-0.4	0.7 to 0.9	0.8		-	-
II	1401-44	L	Ca	1	4	S	L-rich	240-247	242	-0.2 to -0.3	-0.2	0.4 to 0.5	0.4		-	-
II	905-167	L	Qtz	2	6	S	L-rich	209-224	217	-0.6 to -0.8	-0.7	1.1 to 1.4	1.2		-	-
II	905-127	L	Qtz	2	4	S	L-rich	197-204	200	-0.5 to -0.6	-0.6	0.9 to 1.1	1		-	-
II	1301-31	K	Qtz	4	5	S	L-rich	201-202	201	-0.3 to -0.8	-0.6	0.5 to 1.4	1		-	-
II	1401-31	K	Qtz	6	4	S	L-rich	189-190	189	-3.1 to -3.4	-3.3	5.1 to 5.6	5.4		-	-
III	DM12	M	Ca	1	5	S	L + illite	173-178	175	-0.2 to -0.3	-0.3	0.4 to 0.5	0.5		-	-
III	DM12	M	Ca	2	9	S	L + illite	172-179	176	-0.2 to -0.3	-0.3	0.4 to 0.5	0.5		-	-
III	DM12	M	Ca	4	6	S	L + illite	170-173	171	-0.2 to -0.3	-0.3	0.4 to 0.5	0.5		-	-
III	DM12	M	Ca	1	8	S	L + illite	155-164	160	-0.2 to -0.3	-0.2	0.4 to 0.5	0.4		-	-
III	DM10	M	Ca	1	5	S	L + illite	179-184	181	-0.2 to -0.3	-0.3	0.4 to 0.5	0.5		-	-
III	DM12	M	Ca	2	6	S	L + illite	169-175	171	0 to -0.1	-0.1	0 to 0.2	0.1		-	-
III	1105-208	TM	Qtz	1	8	S	L+V	200-204	202	-0.8 to -0.9	-0.9	1.4 to 1.6	1.5	171	122	899
III	1105-210	TM	Ca	2	5	S	L-rich	186-196	192	-0.2 to -0.3	-0.3	0.4 to 0.5	0.5		-	-
III	1405-264	I	Ca	1	5	S	L + illite	193-203	198	-0.2 to -0.3	-0.3	0.4 to 0.5	0.5		-	-
III	1405-272	ND	Qtz	1	3	S	L-rich	169-185	179	-0.4 to -0.4	-0.4	0.7 to 0.7	0.7		-	-
III	1405-272	ND	Qtz	2	4	S	L-rich	173-184	178	-0.5 to -0.9	-0.7	0.9 to 1.6	1.1		-	-
III	1405-272	ND	Qtz	3	5	S	L-rich	170-172	170	-0.4 to -0.4	-0.4	0.7 to 0.7	0.7		-	-
III	1405-271	ND	Qtz	2	5	S	L-rich	187-194	191	-0.3 to -0.7	-0.5	0.5 to 1.2	0.8		-	-
III	1305-272	ND	Qtz	1	6	S	L-rich	163-165	164	-0.5 to -0.6	-0.6	0.9 to 1.1	1		-	-
III	1305-272	ND	Qtz	2	8	S	L-rich	207-210	209	-0.4 to -0.5	-0.4	0.7 to 0.9	0.8		-	-
III	1405-272	ND	Qtz	1	8	S	L-rich	161-174	166	-0.3 to -0.4	-0.3	0.5 to 0.7	0.6		-	-
III	1305-265	ND	Qtz	1	5	S	L-rich	194-200	198	-0.5 to -0.7	-0.6	0.9 to 1.2	1		-	-
III	1305-265	ND	Qtz	3	6	S	L-rich	198-205	200	-0.3 to -0.4	-0.4	0.5 to 0.7	0.6		-	-
III	1305-265	ND	Qtz	4	8	S	L-rich	199-202	200	0 to -0.1	-0.1	0 to 0.2	0.1		-	-
III	1305-265	ND	Qtz	1	10	S	L-rich	198-200	199	-0.6 to -0.7	-0.6	1.1 to 1.2	1.1		-	-
III	1305-265	ND	Qtz	3	4	S	L-rich	190-197	193	-0.6 to -0.7	-0.7	1.1 to 1.2	1.1		-	-
III	305-05	ND	Qtz	1	4	S	L + illite	206-209	208	-1.4 to -1.5	-1.5	2.4 to 2.6	2.5		-	-
III	1405-266	ND	Qtz	3	7	S	L-rich	167-168	167	-0.3 to -0.4	-0.4	0.5 to 0.7	0.6		-	-
III	140-135	B	Ca	1	4	S	L + illite	185-190	187	-0.5 to -0.6	-0.5	0.9 to 1.1	0.9		-	-
III	905-140	L	Qtz	2	2	P	L-rich	189-192	191	-0.8 to -0.9	-0.9	1.4 to 1.6	1.5		-	-
III	905-125	L	Qtz	1	2	S	L-rich	190-199	194	-0.5 to -0.6	-0.6	0.9 to 1.1	1		-	-
III	1401-34	D	Ca	8	4	S	L-rich	180-185	182	-0.3 to -0.7	-0.5	0.5 to 1.2	0.8		-	-
III	1305-251	D	Ca	1	6	S	L + illite	218-220	219	-0.6 to -0.7	-0.7	1.1 to 1.2	1.1		-	-
III	1305-251	D	Ca	2	5	S	L + illite	218-220	219	-0.6 to -0.7	-0.6	1.1 to 1.2	1.1		-	-
III	1305-254	D	Ca	1	5	S	L-rich	182-196	190	-0.9 to -1.1	-1	1.6 to 1.9	1.7		-	-
IV	Oct_2011_1056563	P	Qtz	2	2	S	L+V	275-289	282	-0.4 to -0.6	-0.5	0.7 to 1.1	0.9	798	0	273
IV	905-178	P	Ca	1	4	P	L-rich	190-195	192	-0.7 to -0.8	-0.8	1.2 to 1.4	1.3		-	-
IV	Oct_2011_1056561	P	Qtz	1	6	S	L-rich	250-257	254	-0.2 to -0.3	-0.3	0.4 to 0.5	0.4		-	-
IV	Oct_2011_1056561	P	Qtz	2	4	S	L+V	260-265	262	-0.2 to -0.3	-0.2	0.4 to 0.5	0.4	573	0	517

(*continued on next page*)

Paragenetic Stage	Sample no.	Vein	Host	FIA #	n	FI origin (P or S)	FI type	Th range (°C)	Average Th (°C)	Tm range (°C)	Average Tm (°C)	Salinity range (wt.% NaCl)	Average Salinity (wt.%)	Depth of trapping beneath paleosurface based on average Th and salinity	Depth of sample collection (m)	Depth to 300°C Isotherm
IV	705-70	M	Qtz	1	7	S	L+V	227-235	231	0 to -0.1	0	0 to 0.2	0.1	320	0	770
IV	DM10	M	Ca	1	2	S	L-rich	177-178	178	-0.3 to -0.4	-0.4	0.5 to 0.7	0.6		-	-
IV	DM10	M	Ca	2	2	S	L-rich	222-222	222	-0.4 to -0.4	-0.4	0.7 to 0.7	0.7		-	-
IV	DM10	M	Ca	3	2	S	L-rich	179-179	179	-0.3 to -0.3	-0.3	0.5 to 0.5	0.5		-	-
IV	DM5	M	Adu	1	2	S	L-rich	289-289	289	-4.3 to -4.3	-4.3	6.9 to 6.9	6.9		-	-
IV	DM4	M	BCa	1	5	S	L+V	184-192	189	-0.3 to -0.4	-0.4	0.5 to 0.7	0.6	126	132	944
IV	DM4	M	BCa	2	5	S	L+V	159-165	163	-0.4 to -0.5	-0.5	0.7 to 0.9	0.8	62	132	1009
IV	DM7	M	Ca	1	7	S	L+V	182-187	185	-0.4 to -0.6	-0.5	0.5 to 1.1	0.8	114	93	956
IV	DM14	M	Qtz	1	4	S	L+V	215-221	218	-0.4 to -0.5	-0.5	0.7 to 0.9	0.8	242	132	828
IV	DM14	M	Qtz	2	4	S	L-rich	163-174	167	-0.6 to -0.7	-0.6	1.1 to 1.2	1.1		-	-
IV	Oct_2011_1056578	M	Qtz	1	3	S	V-rich	252-263	257	-0.8 to -0.9	-0.8	1.4 to 1.6	1.5		-	-
IV	DM14	M	Qtz	1	3	S	L+V	182-186	184	-0.8 to -0.9	-0.9	1.4 to 1.6	1.5	112	132	959
IV	705-70	M	Qtz	2	2	S	L+V	256-257	257	0 to -0.1	-0.1	0 to 0.2	0.1	524	0	566
IV	Oct_2011_1056551	M	Ca	1	2	S	L-rich	183-193	188	-0.2 to -0.4	-0.3	0.4 to 0.7	0.6		-	-
IV	Oct_2011_1056555	M	Qtz	1	2	S	L+V	270-279	275	-0.2 to -0.4	-0.3	0.4 to 0.7	0.5	720	63	370
IV	Oct_2011_1056555	M	Qtz	1	6	P	L+V	205-217	209	-0.2 to -0.3	-0.3	0.4 to 0.5	0.4	203	63	887
IV	Oct_2011_1056555	M	Qtz	2	2	P	L + illite	250-253	252	0 to -0.1	-0.1	0 to 0.2	0.1		-	-
IV	Oct_2011_1056555	M	Qtz	3	4	P	L + illite	285-290	288	-0.2 to -0.3	-0.3	0.4 to 0.5	0.4		-	-
IV	905-83	M	Qtz	1	4	S	L+V	219-226	223	-0.2 to -0.6	-0.4	0.4 to 1.1	0.7	269	0	802
IV	905-83	M	Qtz	2	1	S	L-rich	225-225	225	-0.1 to -0.3	-0.2	0.2 to 0.5	0.4		-	-
IV	905-83	M	Qtz	5	6	S	L+V	225-235	230	-0.2 to -0.3	-0.2	0.4 to 0.5	0.4	314	0	776
IV	905-83	M	Qtz	6	8	S	L+V	218-240	230	-0.6 to -0.9	-0.8	1.1 to 1.6	1.4	310	0	761
IV	DM3	M	BCa	1	5	S	L+V	183-192	188	-0.4 to -0.5	-0.5	0.7 to 0.9	0.8	123	161	947
IV	1105-205	M	Ca	1	6	S	L+V	180-181	181	-0.4 to -0.5	-0.5	0.4 to 0.7	0.5	105	92	985
IV	1405-264	I	Qtz	1	11	S	L + illite	280-291	287	-0.4 to -0.7	-0.5	0.7 to 1.2	1			
IV	1405-264	I	Qtz	2	6	S	L + illite	288-291	290	-0.4 to -0.7	-0.5	0.7 to 1.2	0.9		-	-
IV	1305-272	ND	Qtz	3	7	S	L+V	180-194	191	-0.4 to -0.5	-0.4	0.7 to 0.9	0.8	133	254	938
IV	1305-265	ND	Qtz	2	2	S	L+V	194-195	195	-0.5 to -0.6	-0.6	0.9 to 1.1	1	146	254	925
IV	1305-265	ND	Qtz	4	7	S	L-rich	190-201	195	-0.5 to -0.8	-0.7	0.9 to 1.4	1.2		-	-
IV	1305-265	ND	Qtz	5	4	S	L+V	200-209	205	-0.5 to -0.6	-0.5	0.9 to 1.1	0.9	183	254	887
IV	1305-265	ND	Qtz	2	2	S	L+V	220-237	229	-0.2 to -0.3	-0.3	0.4 to 0.5	0.4	308	254	782
IV	1305-265	ND	Qtz	4	5	S	L-rich	200-205	203	-0.5 to -0.6	-0.5	0.9 to 1.1	0.9		-	-

Paragenetic Stage	Sample no.	Vein	Host	FIA #	n	FI origin (P or S)	FI type	Th range (°C)	Average Th (°C)	Tm range (°C)	Average Tm (°C)	Salinity range (wt.% NaCl)	Average Salinity (wt.%)	Depth of trapping beneath paleosurface based on average Th and salinity	Depth of sample collection (m)	Depth to 300°C Isotherm
IV	1405-266	ND	Qtz	1	5	S	L-rich	187-192	190	-0.5 to -0.6	-0.6	0.9 to 1.1	1		-	-
IV	1405-266	ND	Qtz	2	5	S	L+V	222-226	224	-0.4 to -0.5	-0.4	0.7 to 0.9	0.8	274	254	796
IV	1405-271	ND	Qtz	1	8	P	L+V	206-215	211	-0.1 to -0.4	-0.3	0.2 to 0.7	0.5	212	253	878
IV	305-05	ND	Qtz	1	7	S	L+V	211-217	214	-2.1 to -2.8	-2.6	3.5 to 4.6	4.3	213	0	802
IV	305-05	ND	Qtz	2	6	S	L + illite	213-224	219	-1.7 to -1.9	-1.8	2.9 to 3.2	3		-	-
IV	1405-266	ND	Qtz	1	4	S	L+V	328-335	332	-0.5 to -0.6	-0.5	0.9 to 1.1	0.9	1780	254	(-690)
IV	1405-266	ND	Qtz	2	3	S	L+V	190-196	194	-0.2 to -0.3	-0.2	0.4 to 0.5	0.4	145	254	945
IV	705-64	ND	Qtz	1	3	S	L+V	232-235	234	-2.3 to -2.5	-2.4	3.9 to 4.2	4	320	0	695
IV	140-135	B	Ca	1	4	S	L-rich	185-189	188	-0.2 to -0.3	-0.3	0.4 to 0.5	0.4		-	-
IV	1401-41	B	Qtz	1	3	S	L+V	261-263	262	0 to -0.1	-0.1	0 to 0.2	0.1	573	175	517
IV	1401-46	SJ	Qtz	1	2	S	L-rich	296-297	297	-0.1 to -0.2	-0.2	0.2 to 0.4	0.3		-	-
IV	1401-43	L	Ca	1	5	S	L-rich	193-210	202	-0.2 to -0.3	-0.3	0.4 to 0.5	0.5		-	-
IV	905-168	L	Qtz	1	4	S	L+V	212-223	216	-0.6 to -0.8	-0.7	1.1 to 1.4	1.3	236	271	854
IV	905-168	L	Qtz	2	3	S	L+V	210-216	214	-0.8 to -0.9	-0.8	1.4 to 1.6	1.5	226	271	864
IV	1401-44	L	Ca	2	3	S	L-rich	171-182	178	-0.2 to -0.4	-0.3	0.4 to 0.7	0.5		-	-
IV	905-167	L	Qtz	1	3	S	L+V	275-289	282	-0.6 to -0.8	-0.7	1.1 to 1.4	1.2	811	269	279
IV	1401-45	L	Ca	1	4	S	L+V	149-152	151	-0.2 to -0.4	-0.3	0.4 to 0.7	0.5	42	210	1048
IV	1401-45	L	Ca	1	5	S	L + illite	183-185	184	-0.4 to -0.5	-0.5	0.7 to 0.9	0.8		-	-
IV	1401-45	L	Ca	2	5	S	L + illite	187-193	190	-0.3 to -0.5	-0.4	0.5 to 0.9	0.7		-	-
IV	905-168	L	Qtz	1	5	S	L+V	193-219	204	-0.9 to -1.1	-1	1.6 to 1.9	1.8	137	271	914
IV	1401-45	L	Ca	1	6	S	L + illite	185-192	189	-0.2 to -0.5	-0.4	0.4 to 0.9	0.7		-	-
IV	905-153	L	Adu	1	2	S	L-rich	220-221	221	-0.2 to -0.3	-0.3	0.4 to 0.5	0.4		-	-
IV	905-153	L	Ca	2	7	S	L+V	160-164	161	-0.2 to -1.2	-0.8	0.4 to 2.1	1.4	59	163	1031
IV	905-158	L	Ca	1	4	S	L + illite	198-204	201	-0.3 to -0.7	-0.5	0.5 to 1.2	0.8		-	-
IV	905-148	L	Qtz	2	3	S	L+V	254-258	256	-0.3 to -0.6	-0.5	0.5 to 1.1	0.8	515	200	575
IV	1301-31	K	Qtz	1	2	S	L+V	204-205	204	-3.9 to -4.8	-4.4	6.3 to 7.6	6.9	163	0	798
IV	1305-232	K	Ca	1	6	S	L-rich	168-171	170	-0.1 to -0.2	-0.2	0.2 to 0.4	0.2		-	-
IV	1305-232	K	Ca	2	2	S	L-rich	175-178	177	-0.6 to -0.7	-0.7	1.1 to 1.2	1.1		-	-
IV	1305-232	K	Ca	1	3	S	L-rich	170-178	174	-0.7 to -0.8	-0.7	1.2 to 1.4	1.3		-	-
IV	1305-232	K	Ca	3	3	S	L-rich	278-299	290	-0.6 to -0.7	-0.6	1.1 to 1.2	1.1		-	-
IV	1305-260	D	Ca	1	7	S	L+V	181-198	187	-2 to -2.2	-2.1	3.4 to 3.7	3.6	115	115	900
IV	1305-254	D	Qtz	2	3	S	L-rich	223-227	225	-0.7 to -0.9	-0.8	1.2 to 1.6	1.5		-	-

Paragenetic Stage	Sample no.	Vein	Host	FIA #	n	FI origin (P or S)	FI type	Th range (°C)	Average Th (°C)	Tm range (°C)	Average Tm (°C)	Salinity range (wt.% NaCl)	Average Salinity (wt.%)	Depth of trapping beneath paleosurface based on average Th and salinity	Depth of sample collection (m)	Depth to 300°C Isotherm
IV	1301-32	D	Qtz	2	5	S	L+V	225-229	227	-0.4 to -0.6	-0.6	0.7 to 1.1	1	296	0	794
IV	1301-32	D	Qtz	3	4	S	L+V	239-245	241	-0.1 to -0.3	-0.2	0.2 to 0.5	0.4	389	0	701
IV	1305-260	D	Qtz	1	6	S	L+V	177-188	182	-1.9 to -2	-2	3.2 to 3.4	3.3	101	115	932
IV	905-163	OV	Ca	1	2	S	L+V	208-211	210	-0.2 to -0.3	-0.3	0.4 to 0.5	0.4	208	105	882
V	578	M	Ca	1	2	S	L-rich	137-138	138	-0.7 to -0.8	-0.8	1.2 to 1.4	1.3		-	-
V	DM12	M	Ca	2	2	P	L-rich	188-188	188	-0.1 to -0.2	-0.2	0.2 to 0.4	0.3		-	-
V	1105-215	I	Ca	1	9	P	L-rich	189-203	198	-0.1 to -0.3	-0.2	0.2 to 0.5	0.4		-	-
V	1401-37	B	Ca	5	7	S	L-rich	234-249	240	-0.4 to -0.5	-0.5	0.7 to 0.9	0.8		-	-
V	1401-38	B	Ca	7	7	S	L-rich	209-216	210	0 to -0.4	-0.1	0 to 0.7	0.3		-	-
V	1401-38	B	Ca	8	2	S	L-rich	208-209	208	-0.4 to -0.4	-0.4	0.7 to 0.7	0.7		-	-
V	905-140	L	Ca	1	3	S	L-rich	225-227	226	0 to -0.1	0	0 to 0.2	0.1		-	-
V	1305-255	K	Ca	1	2	S	L-rich	146-148	147	-0.2 to -0.3	-0.3	0.4 to 0.5	0.4		-	-

S= secondary fluid inclusions; P= primary fluid inclusions; Th= homogenization temperature
Tm= ice melting temperature; n= number of fluid inclusion in the FIA
L-rich = liquid-rich inclusions with consistent liquid-to-vapor ratios; LV= coexisting liquid-rich and vapor-rich inclusions
L + illite = liquid-rich inclusions with consistent liquid-to-vapor ratios and containing a trapped illite crystal; V-rich= assemblages consisting of only vapor-rich inclusions
Ca = Calcite; Qtz = Quartz; BCa = Bladed calcite; Adu = Adularia
B = Bolañitos; D = Daniela; I = Intermediate; K = Karina; L = Lucero; M = Melladito
ND = Nombre de Dios; OV = Other_vein; Per = Perpendicular; P = Plateros
SJ = San Jose; TM = Traverse Melladito

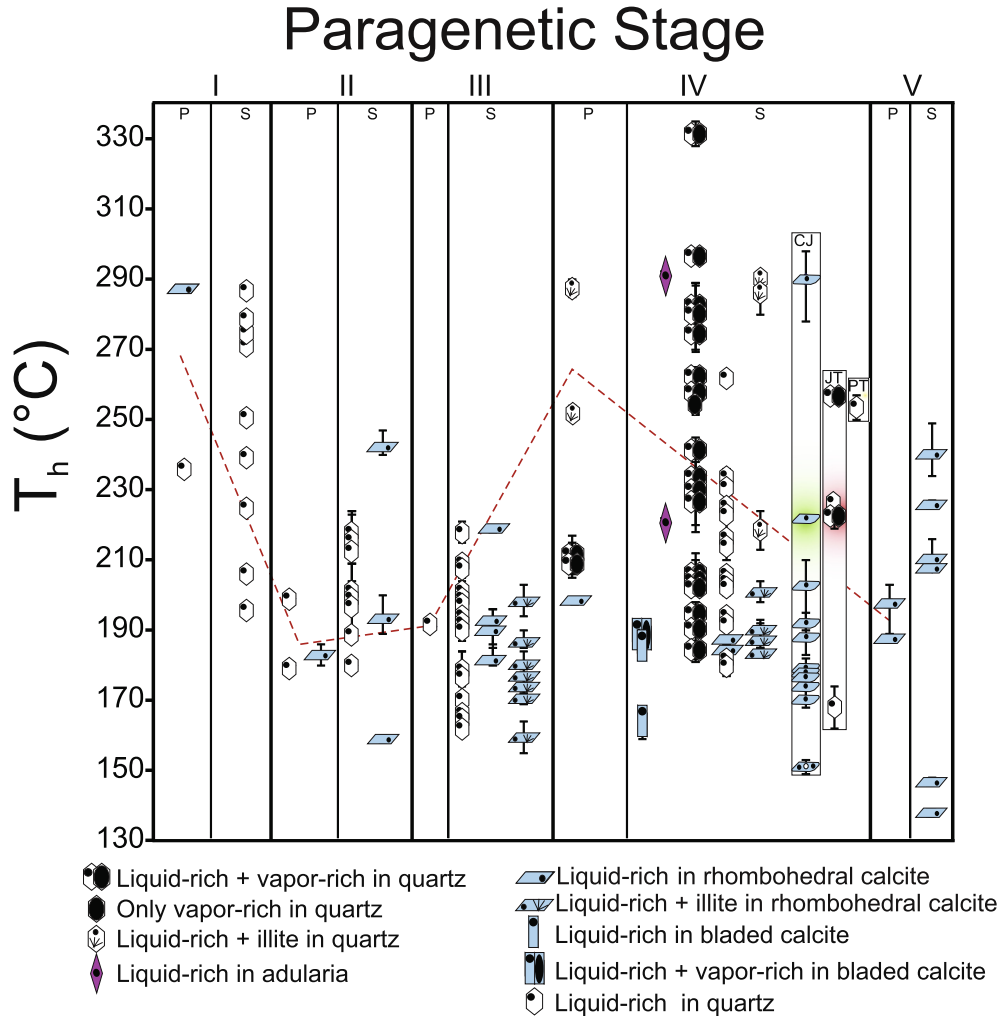

Fig. 16. Distribution of fluid inclusion types and homogenization temperatures as function of paragenetic stage for samples from the La Luz vein system at Guanajuato, Mexico. "P" represents primary fluid inclusions, and "S" represents secondary fluid inclusions. In Stage IV CJ = calcite containing secondary inclusions and cemented by jigsaw quartz; JT = secondary fluid inclusions cutting jigsaw quartz; PT = secondary fluid inclusions cutting plumose texture quartz. The dashed red line represents the average homogenization temperatures of primary fluid inclusions in the different stages.

vein formation. Accordingly, if the depositional mechanism is boiling, and if the fluid PT conditions remain on the boiling curve from the depth at which boiling begins all the way to surface as suggested by many previous studies, then the depth at which boiling began is represented by the depth at which the sample was collected or some greater depth. Assuming 300 °C as a reasonable temperature for initiation of boiling, the depth at which boiling began is easily approximated using the method of Haas (1971).

7.2.1. Plateros vein

The homogenization temperatures (T_h) of FI from the Plateros vein range from 187 to 289 °C. Primary Fluid Inclusion Assemblages (FIAs) in rhombohedral calcite contain liquid-rich fluid inclusions with T_h of 190–195 °C. Secondary FIAs crosscutting jigsaw texture quartz consist of coexisting liquid-rich and vapor-rich fluid inclusions with T_h from 260 to 289 °C. Two samples from the Plateros vein (samples Oct_2011_1056561 and Oct_2011_1056563; Table A1) collected from the surface contain FIAs with coexisting liquid-rich and vapor-rich inclusions. Based on homogenization temperatures of liquid-rich inclusions from these FIAs and assuming that the fluid remained on the boiling curve to the surface (or to the paleo-water table), the fluid inclusions would have been trapped at depths of 573 and 798 m beneath the paleo-surface (Tables 1, A1), and the 300 °C isotherm would have been located 273 and 517 m, respectively, beneath the present surface (Table 1).

7.2.2. Melladito vein

Several fluid inclusion assemblages hosted in a wide range of minerals were measured from the Melladito vein (Tables 1; A1). Several FIAs indicate the presence of boiling, including, secondary FIAs consisting of coexisting liquid-rich and vapor-rich FI hosted in rhombohedral calcite that show T_h from 182 to 187 °C; secondary FIAs consisting of coexisting liquid-rich and vapor-rich fluid inclusions in bladed calcite with T_h from 184 to192 °C; primary FIAs with coexisting liquid-rich and vapor-rich fluid inclusions with T_h from 205 to 217 °C in euhedral quartz; secondary FIAs of coexisting liquid-rich and vapor-rich fluid inclusions with T_h from 182 to 279 °C in jigsaw quartz; secondary FIAs with only vapor-rich fluid inclusions in jigsaw quartz showing T_h from 252 to 263 °C.

Fifteen FIAs from the Melladito vein show evidence of boiling in the form of coexisting liquid-rich and vapor-rich fluid inclusions (Table A1). Five of the FIAs were in samples collected from the surface, three were from in underground workings, and seven were from drill core samples. The estimated depth to the 300 °C isotherm on the Melladito vein from the present surface ranges from 370 to 1009 m (Table 1). These depths are greater than the deepest sampling depths. Assuming that the fluid remains on the boiling curve to 300 °C, the bottom of the boiling zone occurs at depths greater than the maximum depth sampled to date.

7.2.3. Intermediate vein

Homogenization temperatures of FI from the Intermediate vein range from 158 to 291 °C (Tables 1; A1). Primary, liquid-rich FIAs in rhombohedral calcite show T_h from 189 to 203 °C. and secondary FIAs containing liquid-rich inclusions show T_h from 158 to 160 °C. Secondary FIAs containing liquid-rich inclusions with trapped illite in rhombohedral calcite and in euhedral quartz show T_h from 193 to 203 °C and from 280 to 291 °C, respectively. No FIAs consisting of coexisting liquid-rich and vapor-rich fluid inclusions were observed in samples from the Intermediate vein and, therefore, the depth to the 300 °C isotherm could not be calculated.

7.2.4. Nombre de Dios vein

The Nombre de Dios vein samples show T_h ranging from 161 to 335 °C (Tables 1; A1). Eleven FIAs with coexisting liquid-rich and vapor-rich fluid inclusions were observed – two were in surface samples and nine were from drill cores. The FIAs with coexisting liquid-rich and vapor-rich fluid inclusions include primary inclusions in euhedral quartz with T_h from 206 to 215 °C, and secondary FIAs in euhedral quartz with T_h from 180 to 335 °C. Two samples collected from different locations along the vein at the surface show homogenization temperatures ranging from 211 °C to 235 °C. The depth to the 300 °C isotherm calculated from the microthermometric data ranges from 695 to 945 m (Table 1). One sample from stage IV in the paragenesis (the gold-silver stage) contains a FIA consisting of four inclusions with consistent T_h from 328 to 335 °C – for this FIA the predicted depth to the 300 °C isotherm is negative (Table 1), i.e., it would be located above the present ground surface.

7.2.5. Bolañitos vein

Homogenization temperatures of FI from the Bolañitos vein range from 185 to 263 °C (Tables 1, A1). Secondary FIAs containing liquid-rich inclusions in rhombohedral calcite show a T_h range from 185 to 249 °C, and secondary FIAs with liquid-rich inclusions with trapped illite in this phase show T_h from 185 to 190 °C. Coexisting liquid-rich and vapor-rich fluid inclusions in jigsaw quartz show a T_h range from 261 to 263 °C. This sample was collected in the Bolañitos Mine at a depth of ~175 m beneath the present surface. The predicted depth to the 300 °C isotherm beneath the present surface is 517 m (Table 1), or ~342 m beneath the depth in the mine where the sample was collected.

7.2.6. San José vein

The San José vein contains FIAs consisting of only vapor-rich FI and FIAs consisting of liquid-rich FI in jigsaw quartz that show T_h ranging from 296 to 297 °C. The depth to 300 °C isotherm was not calculated for the San José vein because coexisting liquid-rich and vapor-rich fluid inclusions were absent.

7.2.7. Lucero vein

The homogenization temperatures of FI from the Lucero vein range from 171 to 247 °C (Tables 1; A1). Primary, liquid-rich FIAs in rhombohedral calcite show T_h ranging from 199 to 200 °C. Secondary FIAs consisting of liquid-rich FI in rhombohedral calcite show a T_h range from 171 to 247 °C. Secondary FIAs consisting of coexisting liquid-rich and vapor-rich FI hosted in rhombohedral calcite show a T_h range from 193 to 247 °C. Secondary FIAs with liquid-rich inclusions with trapped illite in rhombohedral calcite contain show a T_h range from 183 to 204 °C. Primary, liquid-rich FIAs in quartz euhedral show a T_h range from 189 to 192 °C. Secondary, liquid-rich FIAs in euhedral quartz show a T_h range from 190 to 224 °C. Secondary FIAs consisting of coexisting liquid-rich and vapor-rich FI in jigsaw texture quartz show a T_h range from 193 to 289 °C. Secondary, liquid-rich FIAs in adularia show a T_h range from 220 to 221 °C. Fragments of rounded rhombohedral calcite surrounded by jigsaw texture quartz contain secondary, liquid-rich FIAs with T_h ranging from 171 to 210 °C. One sample with fragments of rounded rhombohedral calcite surrounded by jigsaw texture quartz contains secondary FIAs with coexisting liquid-rich and vapor-rich inclusions with a broad range in liquid-to-vapor ratios and T_h range from 149 to 152 °C.

Eleven FIAs from the Lucero vein contain coexisting liquid-rich and vapor-rich FI (Tables 1; A1). The depth beneath the paleosurface required for the fluid to be on the liquid-vapor curve for the measured average homogenization temperature and salinity ranges from 42 to 811 m, and the depth beneath the current sur-

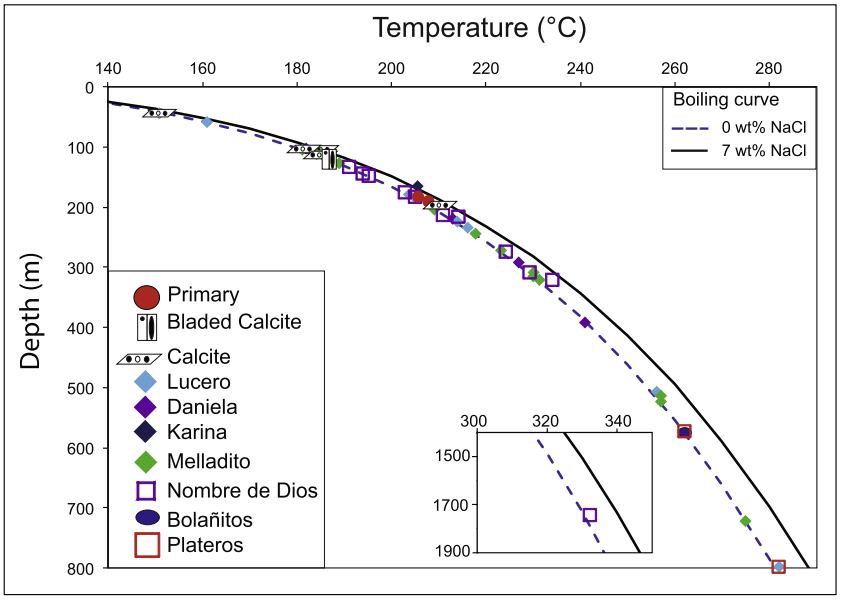

Fig. 17. Homogenization temperatures of liquid-rich inclusions from FIAs consisting of coexisting liquid-rich and vapor-rich inclusions, plotted on the boiling point with depth curves for salinities of 0 and 7 wt.% NaCl, which represents the total range in salinity for all inclusions from the La Luz vein system. The filled red dots represent primary inclusions; all other fluid inclusions are secondary. Note that each data point represents the average homogenization temperature for an individual Fluid Inclusion Assemblage consisting of two or more fluid inclusions that were trapped at the same time. The boiling point with depth curves were calculated according to Haas (1971).

face corresponding to the 300 °C isotherm on the Lucero vein ranges from 279 to 1048 m (Table 1).

7.2.8. Karina vein

Homogenization temperatures of FI in samples from the Karina vein range from 146 to 299 °C (Tables 1; A1). Secondary, liquid-rich FIAs in rhombohedral calcite show a T_h range from 146 to 148 °C. Secondary, liquid-rich FIAs in jigsaw quartz show a T_h range from 189 to 202 °C. Fragments of rounded, rhombohedral calcite surrounded by jigsaw quartz contain secondary liquid-rich FIAs with T_h ranging from 168 to 299 °C. Secondary FIAs consisting of coexisting liquid-rich and vapor-rich FI in jigsaw quartz show a T_h range from 204 to 205 °C. The depth beneath the paleo-surface required for the fluid to be on the liquid-vapor curve for the measured average homogenization temperature and salinity is 163 m, and the depth beneath the current surface to the 300 °C isotherm is 798 m (Table 1).

7.2.9. Daniela vein

The Daniela vein shows a T_h range from 177 to 245 °C (Tables 1; A1). Secondary, liquid-rich FIAs in rhombohedral calcite show a T_h range from 180 to 196 °C. Secondary FIAs consisting of coexisting liquid-rich and vapor-rich fluid inclusions in rhombohedral calcite show a T_h range from 181 to 222 °C. Secondary FIAs with liquid-rich inclusions with trapped illite in rhombohedral calcite show a T_h range from 218 to 220 °C. Secondary liquid-rich FIAs in jigsaw quartz show a T_h range from 223 to 227 °C. Secondary FIAs consisting of coexisting liquid-rich and vapor-rich FI in jigsaw quartz show a T_h range from 177 to 245 °C, corresponding to trapping depths beneath the paleo-surface ranging from 101 to 389 m (Table 1). The depth beneath the present surface to the 300 °C isotherm based on these data ranges from 701 to 932 m (Table 1).

7.2.10. Distribution of fluid inclusion types within the paragenesis

The types of fluid inclusions observed and microthermometric behavior show systematic variations depending on the stage within the paragenesis. The fluid inclusion data for the different stages are summarized in Fig. 16 and Table 1.

Stage I is represented by a compressional tectonic event in the Cretaceous that generated structures oriented 240° (NE-SW), or perpendicular to the main NW-SE trend of the La Luz vein system. All fluid inclusions in this stage are liquid-rich. Assemblages consisting of coexisting liquid-rich and vapor-rich inclusions, or only vapor-rich inclusions, are absent. Homogenization temperatures range from about 200–290 °C, and salinities are typically <1 wt.% NaCl equivalent (Table 1).

Paragenetic stages II and III were produced during extension in the Eocene prior to mineralization. Pyrite with traces of gold and silver in stockwork mineralization occurs late in Stage III. As with Stage I, all fluid inclusions in Stage II are liquid-rich. Homogenization temperatures for Stage II are relatively low, ranging from about 180 to 240 °C (Table 1). Salinities are typically <2 wt.% NaCl equivalent, with one anomalous FIA with salinities ranging from 5.1 to 5.6 wt.% NaCl equivalent (n = 6) (Table 1).

Stage III is the first stage in the paragenesis in which evidence of boiling is observed, based on the presence of a single FIA composed of coexisting liquid-rich and vapor-rich inclusions. Liquid-rich inclusions with trapped illite are also present in this stage – this is a feature that we associate with a transition from non-boiling to boiling conditions, with non-boiling fluids in equilibrium with quartz and illite, and boiling fluids in equilibrium with amorphous silica and adularia (Fig. 4). Homogenization temperatures for Stage III range from about 160 to 220 °C (Table 1). Salinities are typically <2 wt.% NaCl equivalent, with one FIA having salinities ranging from 2.4 to 2.6 wt.% NaCl equivalent (n = 4) (Table 1). The single FIA containing coexisting liquid-rich and vapor-rich FI showed homogenization temperatures of 200–204 °C (n = 8) and salinity of 1.5 wt.% NaCl equivalent.

Stage IV represents the Ag-Au stage and shows the strongest FI evidence for boiling. While FIAs with coexisting liquid-rich and vapor-rich FI were not observed in Stages I or II, and only one such assemblage was observed in Stage III, 38 out of 69 FIAs analyzed from Stage IV contain coexisting liquid-rich and vapor-rich FI (Table 1). Homogenization temperatures for Stage IV were noticeably higher than those obtained for FIAs in earlier stages. While the lower end of the T_h range was essentially the same in all stages at about 160–170 °C, many more FIAS in Stage IV showed elevated

average T_h values, with ten FIAs having average $T_h \geq 275$ °C (Table 1). One FIA consisting of coexisting liquid-rich and vapor-rich FI had an average T_h of 332 °C (n = 4; range from 328 to 335 °C), representing the highest temperature observed in this study. Salinities are typically < 2 wt.% NaCl equivalent, with a few FIAs having salinities >3 wt.% NaCl equivalent and one with a salinity of 6.9 wt.% (Table 1).

All fluid inclusions in post-mineralization Stage V occur within rhombohedral calcite. All FIAs were composed of liquid-rich inclusions with homogenization temperatures ranging from about 140 to 240 °C, and salinities <1 wt.%, except for one FIA with salinity of 1.3 wt.% (Table 1).

8. Implications for exploration in the La Luz area

In discussing exploration criteria for epithermal systems, Simmons and Browne (2000) state "*... the main features that assist the explorer in resolving the location of paleozones of boiling upflow, and thus promising exploration targets in low-sulfidation epithermal environments, include.... platy calcite (or more commonly its quartz pseudomorph), adularia, and crustiform – colloform silica banding in veins is clear evidence of paleozones of boiling upflow by chloride waters. Precious metal mineralization typically occurs in their vicinity.*" Simmons et al. (2005) similarly report "*Boiling occurs in the central upflowing column of fluid down to 1- to 2-km depth below the water table, controlled by near-hydrostatic pressure–temperature conditions (Fig. 4). In this environment, quartz, adularia, and calcite (usually platy) deposit in open spaces and subvertical channels from the boiling and cooling liquid*". White and Hedenquist (1995) note that "*The most favorable site for mineralization will probably be found associated with the upflow zone*". Accordingly we associate areas that show the strongest evidence of boiling along the various veins in the La Luz area to represent locations that should be given priority during exploration. Moreover, we also suggest that if the depth to the 300 °C isotherm is greater than the depth that has been sampled in areas showing evidence of boiling, additional resources may be found beneath these explored areas.

In the La Luz area some veins that are wide and mineralized at depth do not outcrop at the surface, or are thin and/or intermittent along strike. In addition, thin intermittent veins often parallel the main vein at distances up to several 10 s of meters laterally. In such cases, evidence of boiling is often observed in these small fractures and veins, providing evidence that a wider vein may be present at depth or may outcrop in the area where the smaller veins are found. Typically, samples from the peripheral veinlets show low and erratically distributed metal grades and, thus, might not be given high-priority based on metal grades alone. However, if boiling textures are observed in outcrop or hand sample (as well as features that can only be recognized under the microscope) the area should not be abandoned without some further examination. In a similar manner, we observe that many drill core samples in the La Luz area show good evidence of boiling several tens of meters before the main vein is intersected, as demonstrated for drill hole DDH-1 in the Melladito vein (Fig. 18). Again, this evidence suggests that continued drilling for some additional 10 s of meters may prove fruitful.

As noted above, small veinlets typically occur parallel to the main mineralized veins in the La Luz district and locally occur up to a few hundred meters on both sides of the main vein. Samples of these small veinlets were collected parallel to the Mellidito vein at La Luz and examined. Although Au and Ag grades in the samples collected away from the main vein are generally low and vary in an erratic manner, the samples show good evidence of boiling (Fig. 19). Thus, the presence of such small veins with low metal grades but showing evidence of boiling provides clues that a larger vein may be located nearby, even though that larger vein might not crop out at the surface.

Results of the textural and fluid inclusion data from this study are summarized on the longitudinal section shown in Fig. 20. Plotted here are samples with Boiling Confidence Factors of 5 or greater, along with those samples that contain >1 ppm Au, >100 ppm Ag (or both). Also shown is the calculated depth to the 300 °C isotherm for all samples that contain coexisting liquid-rich and vapor-rich fluid inclusions, and with consistent homogenization temperatures of the liquid-rich inclusions. As shown on Fig. 20, many samples that show elevated BCF have low concentrations of both Au and Ag. The presence of boiling, but without significant Au or Ag, could indicate that metal precipitation occurred at depth. As the depth to the 300 °C isotherm is well below the depths at which the samples were collected, and deeper than the greatest depths that have been explored, undiscovered

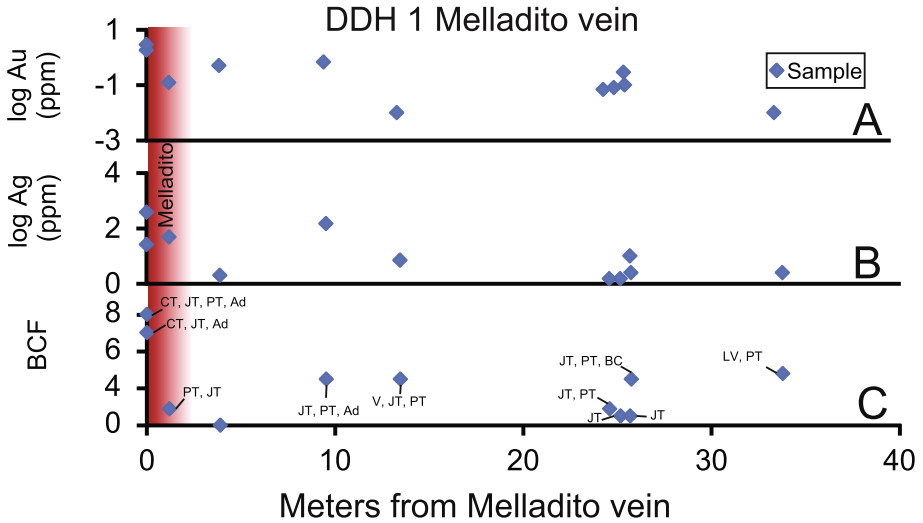

Fig. 18. Concentrations of gold (A) and silver (B), and the Boiling Confidence Factor (C) of samples from drill hole DDH 1 as a function of distant from the Melladito vein (vein shown in red on left side of diagram). Note that samples collected away from the vein show evidence of boiling, even though the gold and/or silver values may be low. CT = colloform quartz; JT = jigsaw quartz; PT = plumose quartz; V = assemblages consisting of only vapor-rich inclusions; LV = assemblages consisting of coexisting liquid-rich and vapor-rich inclusions; Ad = adularia; BC = bladed calcite or bladed calcite replaced by quartz.

economic mineralization may be present at depth and should be given consideration during exploration.

It is worth noting that the depth of trapping of FIAs consisting of coexisting liquid-rich and vapor-rich fluid inclusions, i.e., fluid inclusions trapped on the liquid-vapor (or boiling) curve (Fig. 17; Table 1) is sometimes less than the current depth at which the sample was collected. This observation suggests that either additional rock material was deposited on top of the La Luz system after formation of the fluid inclusions (and after mineralization), or that a simple hydrostatic model based on the PVTX properties of the system H_2O-NaCl is inadequate to describe the temperature-pressure-(depth) relationships of the fluid inclusions. Geological evidence for additional deposition post-mineralization is absent, and this option is not considered to be viable. Using the simple hydrostatic boiling model for H_2O-NaCl is likely the cause of this discrepancy. The presence of breccias in the La Luz lithologies, combined with observations in modern geothermal systems (Hedenquist and Henley, 1985a), indicates that the pressure exceeded normal hydrostatic pressure episodically during the evolution of the system. A pressure gradient higher than that of a conventional hydrostatic gradient would serve to move the calculated depths of formation to shallower levels and could account for the observed discrepancy between calculated depths of formation and current depths of the samples. Alternatively, it is well-known that hydrothermal fluids associated with epithermal mineralization contain small but significant amounts of carbon dioxide (Bodnar et al., 1985; Collins, 1979; Hedenquist and Henley, 1985b). Indeed, it is the loss of CO_2 from the fluid upon boiling that leads to the formation of bladed (platy) calcite (Simmons and Christenson, 1994). Small, undetectable amounts of CO_2 can depress the boiling point with depth curves to greater depths at the same temperature. Thus, the depth corresponding

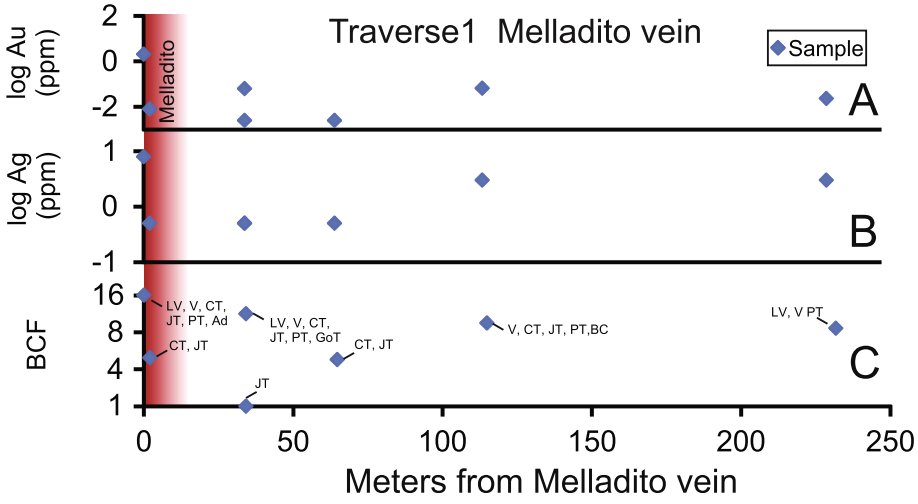

Fig. 19. Surface traverse perpendicular to the Melladito vein in the La Luz vein system at Guanajuato, Mexico showing concentrations of gold (A) and silver (B), and the Boiling Confidence Factor (C) of samples as a function of distant from the vein (vein indicated in red on left side of diagram). Note that samples collected away from the vein show evidence of boiling, even though the gold and/or silver values are sometimes low. CT = colloform quartz; JT = jigsaw quartz; PT = plumose quartz; V = assemblages consisting of only vapor-rich inclusions; LV = assemblages consisting of coexisting liquid-rich and vapor-rich inclusions; Ad = adularia; BC = bladed calcite or bladed calcite replaced by quartz; GoT = Ghost-sphere quartz.

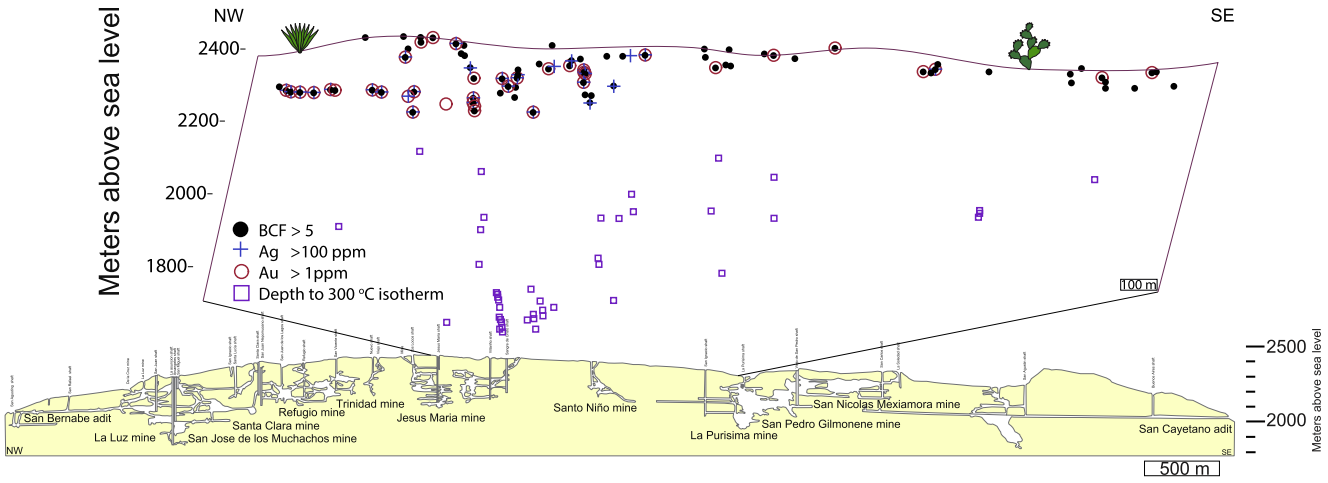

Fig. 20. Summary of mineralogical, textural and fluid inclusion characteristics of samples from the La Luz vein system at Guanajuato, Mexico, plotted on a longitudinal section extending along the vein system from NW to SE. All samples with a Boiling Confidence Factor (BCF) ≥5 are plotted as filled black dots. If the sample also returned >100 ppm Ag, a black plus sign is overlain on the BCF data point. If the sample also returned >1 ppm Au, a red open circle is overlain on the BCF data point. Thus, a black filled circle with a black plus sign and an open red circle overlaying it represents a sample with a BCF of ≥5 that contained both >1 ppm Au and >100 ppm Ag. Also, shown is the calculated depth to the 300 °C isotherm for each Fluid Inclusion Assemblage consisting of coexisting liquid-rich and vapor-rich fluid inclusions. (For interpretation of the references to color in this figure legend, the reader is referred to the web version of this article.)

to a measured homogenization temperature for a CO_2-bearing fluid would be greater than that predicted for CO_2-absent fluids, resulting in a greater calculated depth of formation based on the homogenization temperature. It is likely that the discrepancy between the calculated depths of formation and the current sample depths is a result of both a non-hydrostatic gradient and the presence of small amounts of CO_2 in the fluid. We note, however, that evidence of CO_2 was not detected either during microthermometry or during Raman analysis of the inclusions.

We propose that the use of fluid inclusions and other evidence for boiling is one of many tools that can help the explorationist to identify high priority areas for additional investigation. This assertion is borne out in the Guanajuato Mining District, where earlier studies helped to identify a deep boiling zone on the Veta Madre and led to the eventual discovery of the Au-rich Santa Margarita vein (Moncada and Bodnar, 2012c). According to Great Panther Silver Ltd., the fluid inclusion work has shown that boiling horizons (and associate silver-gold deposition) occur over a vertical range of at least 600 m below the present surface. Similarly, when field work for this study began in the La Luz area, samples were collected from the Lucero vein at the surface. These samples showed strong evidence of boiling and today the Lucerito adit, leading to underground production areas, is located at the location where the samples were collected. We do not suggest that these mineralized zones would not have been discovered in the absence of fluid and textural evidence for boiling. Rather, we offer these examples in support of the use of fluid inclusions and other textural and mineralogical evidence for boiling as one of the tools that should be applied in exploration for epithermal deposits.

In summary, Hedenquist et al. (2000) noted that "The successful exploration geologist uses knowledge of geologic relationships and ore-deposit styles, tempered by experience, to interpret all information available from a given prospect in order to develop an understanding of its mineral potential." Methods to determine whether or not boiling occurred should be included in the explorationist's toolbox because mineralization could be present below the sample collection depth, even if the sample contains little or no metal. Some of this evidence (bladed calcite, colloform quartz, adularia) is easily recognized in hand samples or outcrops, while other evidence (coexisting liquid-rich and vapor-rich fluid inclusions, FIAs containing only vapor-rich inclusions, jigsaw quartz) requires observation under the microscope.

Acknowledgements

The authors acknowledge the continued support from the staff and management at Great Panther Silver Limited and Endeavour Silver Corp. for providing funding for this work, as well as access to properties and data. We especially thank Robert Archer and Robert Brown of Great Panther Silver Limited for their continued support of our research on the Guanajuato Mining District, and Luis R. Castro Valdez of Endeavour Silver for supporting our work at La Luz. Juan José Martínez Reyes shared his knowledge of the Guanajuato Mining District and helped in the field collecting samples. DM acknowledges support from CONACYT 221580.

Appendix A.

Table A1. Sample number, UTM coordinates, elevation, vein identification, collection location (surface, mine, drill core), concentrations of Au, Ag, Cu, Pb, Zn, As, and Sb, and the various textural and fluid inclusion features observed in samples from the La Luz vein system.

Sample Number	UTM X	UTM Y	Elevation (m)	Vein	Collection Location	Au (ppm)	Ag (ppm)	Cu (ppm)	Pb (ppm)	Zn (ppm)	As (ppm)	Sb (ppm)	LV	V	CT	BC	Ad	PT	JT	Gst	**BCF**	L + illite	Rhomb. Calcite	Comb Qtz	Zonal Tex. Qtz
1005-176	246594	2229000	2258	Plateros	Surface	0.01	0.5	30	30	37	19	1	0	0	0	0	0	0	1	0	**1**	0	0	0	0
1005-177	246695	2228903	2225	Plateros	Surface	0.01	0.5	22	0.5	23	26	0.5	0	0	0	0	0	0	1	0	**1**	0	0	0	0
1005-178	246695	2228903	2225	Plateros	Surface	0.30	56	8	0.5	27	14	6	0	0	0	1	1	0	1	0	**7**	0	1	0	0
1005-181	246459	2229100	2309	Plateros	Surface	0.04	5	34	0.5	29	63	3	1	1	1	0	0	1	1	0	**13**	0	0	0	0
1105-188	246751	2228499	2211	Plateros	Surface	0.04	0.5	10	0.5	8		1	0	1	1	0	0	1	1	0	**8**	0	1	0	0
1105-189	246774	2228534	2200	Plateros	Surface	0.01	0.5	48	0.5	20	108	2	0	0	0	0	1	1	0	0	**4**	0	1	0	0
1105-190	246881	2228671	2178	Plateros	Surface	0.18	0.5	19	0.5	10		10	0	0	1	0	1	0	1	0	**7**	0	1	0	0
1105-191	246881	2228671	2178	Plateros	Surface	0.03	1	15	0.5	12		8	0	0	0	0	1	1	0	0	**4**	0	0	0	0
1105-192	246190	2229337	2320	Plateros	Surface	0.01	0.5	2.5	0.5	20	6	1	0	0	0	0	0	0	0	0	**0**	0	1	0	0
1105-193	246093	2229421	2311	Plateros	Surface	0.00	0.5	7	0.5	15	5	0.5	0	1	0	0	0	1	0	0	**4**	0	0	0	0
1105-196	246118	2229493	2320	Plateros	Surface	0.00	0.5	10	0.5	6	3	0.5	0	1	0	0	0	0	1	0	**4**	0	0	0	0
1105-197	246167	2229547	2320	Plateros	Surface	0.00	0.5	2.5	0.5	2.5	10	1	0	0	0	0	1	0	1	0	**4**	0	0	0	0
Oct_2011_1056561	244782	2231367	2400	Plateros	Surface	0.00	2	15	0.5	26	2	0.5	1	0	1	0	0	1	1	0	**10**	0	0	0	0
Oct_2011_1056562	244751	2231491	2398	Plateros	Surface	0.03	0.5	7	0.5	9	0.5	8	0	0	0	0	0	0	1	0	**1**	0	0	0	0
Oct_2011_1056563	244658	2231461	2395	Plateros	Surface	2.85	439	28	10	59	22	6	1	0	1	1	0	0	1	0	**12**	0	0	0	0
Oct_2011_1056572	246885	2228541	2270	Plateros	Underground, La chuparosa	0.03	0.5	17	0.5	7	34	0.5	0	0	0	0	0	0	0	0	**0**	0	0	0	0
Oct_2011_1056573	246894	2228547	2273	Plateros	Underground, La chuparosa	0.05	1	16	0.5	32	50	3	0	0	1	0	0	0	1	0	**4**	0	1	0	0
Oct_2011_1056574	246913	2228553	2271	Plateros	Underground, La chuparosa	0.96	11	2.5	0.5	5	21	3	0	1	0	0	1	0	1	0	**7**	1	1	0	0
Oct_2011_1056575	246938	2228562	2272	Plateros	Underground, La chuparosa	5.01	15	18	0.5	17	37	3	0	1	0	0	1	0	1	0	**7**	1	1	0	0
Oct_2011_1056576	246661	2228931	2240	Plateros	Underground, Chayita	0.11	30	37	10	32	15	3	0	0	1	0	0	1	1	0	**5**	0	1	0	0
Oct_2011_1056577	246681	2228920	2242	Plateros	Underground, Chayita	2.62	89	19	0.5	19	30	6	0	0	0	0	1	1	1	0	**5**	0	1	0	0
305-06	245554	2231874	2350	Melladito	Surface	0.27	26	32	0.5	22	146	3	0	1	1	0	0	1	1	0	**8**	0	0	0	0
305-07	245554	2231874	2350	Melladito	Surface	0.08	4	17	0.5	11	86	2	0	1	0	0	0	1	1	0	**5**	0	0	0	0
705-63	245634	2230780	2333	Melladito	Surface	0.02	3	49	0.5	5	12	3	1	1	0	0	0	1	0	0	**9**	0	0	0	0
705-67	245831	2230655	2373	Melladito	Surface	0.06	0.5	8	0.5	6	166	6	1	1	1	0	0	1	1	1	**14**	0	0	0	0
705-68	245831	2230655	2373	Melladito	Surface	0.00	0.5	13	0.5	9	6	0.5	0	0	0	0	0	0	1	0	**1**	0	0	0	0
705-69	245868	2230648	2368	Melladito	Surface	0.01	0.5	53	0.5	44	13	0.5	0	0	1	0	0	0	1	0	**4**	0	0	0	0
705-70	245866	2230625	2365	Melladito	Surface	2.07	8	80	0.5	18	300	9	1	1	1	0	1	1	1	0	**16**	0	0	0	0
705-71	245930	2230549	2348	Melladito	Surface	0.00	0.5	61	0.5	20	3	0.5	0	0	1	0	0	0	1	0	**4**	0	0	0	0
705-72	245980	2230539	2345	Melladito	Surface	0.07	3	15	0.5	14	47	3	0	1	1	1	0	1	1	0	**11**	0	0	0	0
905-76	246281	2229864	2320	Melladito	Surface	0.07	50	9	0.5	6	6	12	0	0	1	1	0	1	1	0	**8**	0	0	0	0
905-77	246302	2229914	2300	Melladito	Surface	0.02	1	33	0.5	18	65	4	0	0	0	0	0	1	1	0	**2**	0	0	0	0
905-78	246304	2229934	2295	Melladito	Surface	0.21	41	27	0.5	7	300	20	0	0	0	0	0	1	1	0	**2**	0	0	0	0
905-79	246351	2229930	2278	Melladito	Surface	1.94	2	13	0.5	2.5	53	3	1	0	1	1	0	0	0	0	**11**	0	0	0	0
905-80	246392	2229889	2265	Melladito	Surface	0.23	9	39	0.5	6	102	3	0	0	0	0	0	1	1	0	**2**	0	0	0	0
905-81	246387	2229883	2268	Melladito	Surface	0.08	0.5	26	0.5	12	127	0.5	1	0	0	0	0	1	0	0	**6**	0	0	0	0
905-82	246389	2229700	2273	Melladito	Surface	0.56	2	54	0.5	25	179	9	0	0	0	0	0	1	1	0	**2**	0	0	0	0
905-83	246452	2229579	2278	Melladito	Surface	0.02	0.5	6	0.5	10	45	5	1	1	1	0	0	1	1	0	**13**	0	0	0	0
1005-175	246747	2228982	2228	Melladito	Surface	0.01	0.5	91	0.5	67	17	2	0	1	0	0	0	0	1	0	**4**	0	0	0	0
1005-179	246652	2229116	2250	Melladito	Surface	0.02	0.5	7	0.5	15	15	2	0	0	0	0	0	0	1	0	**1**	0	0	0	0
1005-180	246615	2229115	2265	Melladito	Surface	0.08	23	35	0.5	15	67	6	1	1	1	1	0	1	1	0	**16**	0	0	0	0
1105-201	245259	2231472	2318	Melladito	DDH-1	0.10	2.5						1	0	1	1	0	1	1	0	**13**	0	0	0	0
1105-202	245259	2231472	2317	Melladito	DDH-1	0.08	1.5						0	0	0	0	0	0	1	0	**1**	0	1	0	0
1105-203	245275	2231486	2299	Melladito	DDH-1	0.68	149	6	0.5	13	120	14	0	0	0	0	1	1	1	0	**5**	0	1	0	0
1105-204	245280	2231490	2293	Melladito	DDH-1	0.50	2	23	0.5	22	400	3	0	0	0	0	0	0	0	0	**0**	0	1	0	0
1105-205	245284	2231494	2288	Melladito	DDH-1	1.82	26	2.5	0.5	2.5			0	0	1	0	1	0	1	0	**7**	0	1	0	0
1105-206	245285	2231494	2287	Melladito	DDH-1	2.92	385	8	0.5	15	2	19	0	0	0	0	1	0	1	0	**4**	0	1	0	0
1105-207	245286	2231495	2286	Melladito	DDH-1	0.12	49	27	0.5	53	84	5	0	0	0	0	0	1	1	0	**2**	0	1	0	0

(*continued on next page*)

Appendix A. (*continued*)

Sample Number	UTM X	UTM Y	Elevation (m)	Vein	Collection Location	Au (ppm)	Ag (ppm)	Cu (ppm)	Pb (ppm)	Zn (ppm)	As (ppm)	Sb (ppm)	LV	V	CT	BC	Ad	PT	JT	Gst	**BCF**	L + illite	Rhomb. Calcite	Comb Qtz	Zonal Tex. Qtz
1105-208	245310	2231515	2259	Melladito	DDH-1	0.07	1.5						0	0	0	0	0	1	1	0	**2**	0	1	0	0
1105-209	245311	2231516	2258	Melladito	DDH-1	0.29	10	27	0.5	28	189	4	0	0	0	0	0	0	1	0	**1**	0	0	0	0
1105-210	245319	2231523	2248	Melladito	DDH-1	0.01	2.5						1	0	0	0	0	1	0	0	**6**	0	1	0	0
1105-211	245272	2231483	2303	Melladito	DDH-1	0.01	7						0	1	0	0	0	1	1	0	**5**	0	1	0	0
1105-212	245342	2231542	2222	Melladito	DDH-1	0.31	9	35	0.5	38	500	6	0	0	0	0	0	1	1	0	**2**	0	1	0	0
1105-213	245344	2231543	2220	Melladito	DDH-1	0.68	8	36	0.5	36	2	3	0	0	0	0	0	0	0	0	**0**	0	1	0	1
1105-214	245358	2231556	2203	Melladito	DDH-1	0.06	1.5						0	1	1	1	0	1	1	0	**11**	0	1	0	0
1105-216	245357	2231555	2204	Melladito	DDH-1	0.14	3						0	0	0	0	0	0	1	0	**1**	0	1	0	0
1105-217	245363	2231559	2198	Melladito	DDH-1	0.28	6						0	0	0	0	0	0	0	0	**0**	0	0	0	0
1305-267	245234	2231631	2285	Melladito	DDH-9	2.96	35	2.5	20	20	12	6	0	0	1	0	1	0	1	0	**7**	0	0	0	0
1305-268	245232	2231632	2285	Melladito	DDH-14	0.18	6	60	10	90	270	25	0	0	1	0	0	0	1	0	**4**	0	1	0	0
Oct_2011_1056551	245421	2231043	2380	Melladito	Underground, San Pablo	0.15	22	2.5	0.5	2.5	4	2	1	0	1	0	0	1	1	0	**10**	1	1	0	0
Oct_2011_1056552	245422	2231046	2380	Melladito	Underground, San Pablo	2.04	465	24	0.5	22	11	42	1	0	1	0	1	0	1	0	**12**	0	1	0	0
Oct_2011_1056553	245548	2230799	2320	Melladito	Underground, Sangria	0.57	61	7	0.5	12	37	15	0	0	0	0	0	0	1	0	**1**	0	0	0	0
Oct_2011_1056554	245549	2230796	2322	Melladito	Underground, Sangria	0.23	75	9	0.5	8	33	6	0	0	1	0	0	1	1	0	**5**	0	1	0	0
Oct_2011_1056555	245518	2230794	2325	Melladito	Underground, Sangria	8.72	17	7	0.5	2.5	6	1	1	0	1	0	0	1	1	0	**10**	0	1	0	0
Oct_2011_1056556	245315	2231257	2360	Melladito	Underground, Nopal	0.44	75	6	0.5	8	36	8	0	0	1	1	0	1	1	0	**8**	0	0	1	0
Oct_2011_1056557	245241	2231622	2420	Melladito	Surface	0.00	0.5	17	0.5	21	4	0.5	0	0	0	0	0	0	0	0	**0**	0	0	0	0
Oct_2011_1056558	245326	2231367	2405	Melladito	Surface	0.00	1	7	0.5	7	8	0.5	0	0	1	0	0	1	1	0	**5**	0	0	0	0
Oct_2011_1056564	245092	2231769	2396	Melladito	Surface	0.11	9	10	0.5	25	59	8	1	0	1	0	0	0	1	0	**9**	0	1	0	0
Oct_2011_1056565	245094	2231778	2435	Melladito	Surface	0.24	47	26	0.5	31	139	6	0	0	1	1	0	1	1	0	**8**	0	0	0	0
Oct_2011_1056566	245154	2231715	2431	Melladito	Surface	1.44	72	12	0.5	10	16	10	0	0	1	1	0	0	1	0	**7**	0	0	1	0
Oct_2011_1056567	245107	2231917	2435	Melladito	Surface	0.01	0.5	15	0.5	44	9	1	0	0	1	0	0	0	1	0	**4**	0	0	0	0
Oct_2011_1056568	245104	2231925	2430	Melladito	Surface	0.04	3	11	0.5	8	41	11	0	0	1	1	0	1	1	0	**8**	0	0	0	0
Oct_2011_1056569	246905	2228625	2200	Melladito	Underground	0.04	1	19	0.5	11	28	6	0	0	1	0	0	0	1	0	**4**	0	1	0	0
Oct_2011_1056570	246920	2228697	2245	Melladito	Underground	0.04	3	64	0.5	21	49	7	0	0	0	0	0	0	1	0	**1**	0	1	0	0
Oct_2011_1056571	246934	2228711	2240	Melladito	Underground	0.01	0.5	15	0.5	16	16	0.5	0	0	0	0	0	0	1	0	**1**	0	1	0	0
Oct_2011_1056578	246851	2228850	2177	Melladito	Underground, San Jose de abajo	0.07	44	6	0.5	26	300	10	1	1	0	0	0	1	1	0	**10**	0	1	0	0
Oct_2011_1056579	246849	2228849	2177	Melladito	Underground, San Jose de abajo	0.00	5	34	0.5	16	79	3	0	0	1	0	1	1	1	0	**8**	0	1	0	0
Oct_2011_1056581	246751	2229074	2210	Melladito	Underground, San Jose	0.03	23	7	0.5	14	68	8	0	0	0	1	0	1	1	0	**5**	0	1	0	0
Oct_2011_1056582	246973	2228645	2210	Melladito	Underground, San Francisco de Asis	0.52	84	7	0.5	15	38	19	0	0	0	0	0	0	1	0	**1**	0	1	1	0
Oct_2011_1056583	246277	2229874	2297	Melladito	Underground, La Boveda	3.85	350	7	0.5	19	50	23	0	0	0	0	1	0	1	0	**4**	0	1	0	0
Oct_2011_1056584	246278	2229874	2297	Melladito	Underground, La Boveda	1.03	293	2.5	0.5	13	22	28	0	0	1	0	1	0	1	0	**7**	0	1	0	0
Oct_2011_1056584A	246278	2229874	2298	Melladito	Underground, La Boveda	1.03	293	2.5	0.5	13	22	28	0	0	1	0	0	1	1	0	**5**	0	0	0	0
DM3	245291	2231569	2226	Melladito	ESI11-004	0.38	24	14	5	13	182	8	0	0	1	1	0	0	1	0	**7**	1	1	0	0
DM4	245271	2231526	2258	Melladito	ESI11-021	13.70	408	2.5	5	7	11	26	0	0	1	1	1	0	1	0	**10**	0	1	0	0
DM5	245270	2231526	2259	Melladito	ESI10-001	1.82	26	2.5	5	2.5			0	1	1	1	0	1	1	0	**11**	0	1	0	0
DM6	245285	2231494	2288	Melladito	ESI10-001	0.25	28	13	5	27			0	0	0	0	0	0	0	0	**0**	0	0	0	0
DM7	245285	2231494	2287	Melladito	ESI10-001	2.92	385	8	5	15	2	19	1	0	0	0	1	1	1	0	**10**	0	1	0	0
DM8	245291	2231569	2225	Melladito	ESI10-004	0.38	24	14	5	13	182	8	0	0	0	0	1	0	0	0	**3**	0	0	0	0
DM9	245249	2231531	2284	Melladito	ESI11-017	0.20	4.2	3	1	3	86	38	0	0	1	0	0	0	1	0	**4**	0	1	0	0
DM10	245250	2231532	2283	Melladito	ESI11-017	2.36	93	2	1	3	24	81	0	0	1	0	0	0	1	0	**4**	1	1	0	0
DM11	245251	2231533	2282	Melladito	ESI11-017	2.21	156	9	1	3	18	77	0	0	1	1	0	0	1	0	**7**	0	1	0	0
DM12	245270	2231525	2260	Melladito	ESI11-021	7.15	119	19	5	7	20	31	0	0	1	1	0	0	1	0	**7**	1	1	0	0
DM13	245270	2231526	2259	Melladito	ESI11-021	13.70	408	2.5	5	7	11	26	0	0	1	0	1	1	1	0	**8**	0	1	0	0
DM14	245271	2231526	2258	Melladito	ESI11-021	6.88	201	2.5	5	6	26	10	1	0	1	0	1	0	1	0	**12**	0	1	0	0
1105-215	245354	2231552	2208	Melladito	DDH-1	0.96	15	17	0.5	19	0.5	7	0	1	0	0	0	0	1	0	**4**	0	1	0	0
1305-263	245289	2231677	2200	Intermediate	DDH-9	0.34	34	51	0.5	57	0.5	0.5	0	0	1	0	0	0	1	0	**4**	0	0	0	0
1305-264	245290	2231677	2199	Intermediate	DDH-9	2.34	709	17	0.5	39	164	19	0	1	1	0	0	1	1	0	**8**	0	1	0	0

Appendix A. (*continued*)

Sample Number	UTM X	UTM Y	Elevation (m)	Vein	Collection Location	Au (ppm)	Ag (ppm)	Cu (ppm)	Pb (ppm)	Zn (ppm)	As (ppm)	Sb (ppm)	LV	V	CT	BC	Ad	PT	JT	Gst	**BCF**	L + illite	Rhomb. Calcite	Comb Qtz	Zonal Tex. Qtz
1305-269	245287	2231681	2201	Intermediate	DDH-14	0.02	3	60	10	150	170	25	0	0	1	0	0	1	1	0	**5**	0	1	0	0
1305-270	245288	2231681	2199	Intermediate	DDH-14	0.81	83	10	10	20	140	25	1	0	1	0	0	1	1	0	**10**	0	1	0	0
305-02	245517	2232015	2410	Nombre de Dios	Surface	0.78	21	8	0.5	2.5	4	3	0	1	0	1	0	0	1	0	**7**	0	0	0	0
305-03	245517	2232015	2400	Nombre de Dios	Surface	1.14	40	9	0.5	7	5	1	0	1	1	1	0	1	1	0	**11**	0	0	0	0
305-04	245520	2231869	2396	Nombre de Dios	Surface	1.48	162	7	0.5	5	6	4	0	1	1	0	0	1	1	0	**8**	0	0	0	0
305-05	245520	2231869	2395	Nombre de Dios	Surface	0.22	10	11	0.5	10	52	3	0	1	1	0	0	1	1	0	**8**	0	0	0	0
305-08	245565	2231865	2389	Nombre de Dios	Surface	0.02	0.5	7	0.5	2.5	11	1	0	1	1	1	0	0	1	0	**10**	0	0	0	0
705-64	245712	2230888	2362	Nombre de Dios	Surface	0.05	20	35	0.5	6	9	2	1	0	0	0	0	1	1	0	**7**	0	0	0	0
705-65	245814	2230920	2385	Nombre de Dios	Surface	0.02	0.5	14	0.5	7	63	4	0	0	1	0	0	1	1	0	**5**	0	0	0	0
705-66	245851	2230819	2382	Nombre de Dios	Surface	0.00	0.5	40	0.5	46	2	0.5	1	0	0	0	0	0	1	0	**6**	0	0	0	0
705-73	246039	2230518	2355	Nombre de Dios	Surface	0.00	0.5	46	0.5	12	3	0.5	0	0	1	0	0	0	1	0	**4**	0	0	0	0
705-74	246226	2230364	2384	Nombre de Dios	Surface	0.23	8	2.5	0.5	2.5	10	0.5	0	0	0	0	0	0	1	0	**1**	0	0	0	0
705-75	246238	2230378	2386	Nombre de Dios	Surface	2.02	39	9	0.5	2.5	9	6	1	0	1	1	0	1	1	0	**13**	0	0	0	0
1305-265	245321	2231703	2152	Nombre de Dios	DDH-9	8.26	10	18	0.5	27	22	2	1	1	1	0	0	1	1	0	**13**	0	1	0	0
1305-266	245321	2231704	2151	Nombre de Dios	DDH-9	3.03	3	13	0.5	26	11	1	1	1	1	1	0	1	1	0	**16**	0	1	0	0
1305-271	245319	2231708	2153	Nombre de Dios	DDH-14	0.01	1	70	10	80	25	25	1	1	0	0	0	1	0	0	**9**	0	1	0	0
1305-272	245319	2231709	2152	Nombre de Dios	DDH-14	0.00	1	50	10	80	25	25	1	1	1	0	0	1	1	0	**13**	0	1	0	0
1401-35	245201	2232372	2235	Bolañitos	Bolañitos Mine	0.07	9	2.5	5	9	4	0.5	1	1	0	0	0	0	1	0	**9**	0	1	0	0
1401-36	245142	2232116	2242	Bolañitos	Bolañitos Mine	0.71	193	7	5	19	179	46	1	1	1	0	1	1	1	0	**16**	0	1	0	0
1401-36-2	245138	2232113	2242	Bolañitos	Bolañitos Mine	1.00	642	2.5	5	20	28	112	0	0	1	0	1	0	1	0	**7**	0	1	0	0
1401-36-3	245140	2232104	2242	Bolañitos	Bolañitos Mine	2.53	47	6	5	17	60	62	0	0	1	0	1	0	1	0	**7**	0	0	0	0
1401-36-4	245140	2232104	2242	Bolañitos	Bolañitos Mine	0.35	48	2.5	5	9	7	14	0	0	1	0	0	0	1	0	**4**	0	1	0	0
1401-37	245188	2232322	2225	Bolañitos	Bolañitos Mine	44.60	370	6	5	14	15	67	1	0	1	0	1	1	1	0	**13**	0	1	0	0
1401-38	245188	2232328	2225	Bolañitos	Bolañitos Mine	2.38	867	6	5	37	30	35	1	1	1	0	1	1	1	0	**16**	0	1	0	0
1401-39	245176	2232271	2225	Bolañitos	Bolañitos Mine	109.00	2180	98	5	19	23		0	1	1	0	1	1	1	0	**11**	0	1	0	0
1401-40	245172	2232274	2225	Bolañitos	Bolañitos Mine	0.33	73	32	5	14	186	34	0	0	0	0	0	0	1	0	**1**	0	1	0	0
1401-41	245146	2232191	2225	Bolañitos	Bolañitos Mine	7.02	593	6	5	21	24	87	1	1	1	0	1	0	1	0	**15**	0	1	0	0
1401-46	245508	2232246	2197	San Jose	Bolañitos Mine	5.22	3430	138	30	94			0	1	0	0	1	0	1	0	**7**	0	0	0	0
1401-42	245481	2232170	2192	Lucerito	Bolañitos Mine	0.78	87	2.5	5	9	32	43	0	0	1	0	0	0	1	0	**4**	0	1	0	0
1401-42A	245481	2232170	2192	Lucerito	Bolañitos Mine								0	0	0	0	1	0	1	0	**4**	0	1	0	0
1401-43	245473	2232187	2195	Lucerito	Bolañitos Mine	22.80	6780	140	30	101	24		0	1	1	0	1	0	1	0	**10**	0	1	0	0
1401-44	245505	2232075	2195	Lucerito	Bolañitos Mine	0.43	68	2.5	5	2.5	52	44	1	1	0	0	0	0	1	0	**9**	0	1	0	0
1401-45	245503	2232076	2195	Lucerito	Bolañitos Mine	2.59	1120	2.5	10	28	12	136	1	0	1	0	0	1	1	0	**10**	1	1	0	0
1401-47	245498	2232092	2175	Lucerito	Bolañitos Mine	1.08	181	8	5	14	45		0	0	1	0	0	0	1	0	**4**	0	1	0	0
905-124	245593	2231616	2113	Lucerito	DDH-LC-03	0.77	85						0	0	0	0	0	0	1	0	**1**	0	1	0	0
905-125	245593	2231616	2111	Lucerito	DDH-LC-03	2.88	525						0	0	1	0	1	1	1	0	**8**	1	1	0	0
905-127	245593	2231615	2109	Lucerito	DDH-LC-03	0.00	2.5						1	1	0	0	0	1	1	0	**10**	0	0	1	0
905-139	245449	2232047	2114	Lucerito	DDH-LC-26	5.40	194						0	1	1	0	1	1	1	0	**11**	0	1	0	0
905-140	245449	2232047	2114	Lucerito	DDH-LC-26	5.40	194						1	0	0	0	1	1	1	0	**10**	0	1	0	0
905-148	245755	2231431	2171	Lucerito	DDH-LC-29	0.39	2.5						0	0	1	0	1	0	1	0	**7**	0	1	0	0
905-153	245849	2231362	2209	Lucerito	DDH-LC-31	0.68	351						0	1	1	0	1	1	1	0	**11**	0	1	0	0
905-157	245501	2231937	2149	Lucerito	DDH-LC-20	1.91	27						0	0	1	0	0	0	1	0	**4**	0	1	0	0
905-158	245501	2231937	2150	Lucerito	DDH-LC-20	0.79	23						0	0	0	0	1	0	1	0	**4**	1	1	0	0
905-165	245526	2231834	2140	Lucerito	DDH-LC-15	0.23	53						0	0	0	1	1	1	1	0	**8**	0	1	0	0
905-166	245527	2231835	2137	Lucerito	DDH-LC-15	2.73	151						0	1	1	0	1	0	1	0	**10**	0	1	0	0
905-167	245527	2231835	2136	Lucerito	DDH-LC-15	1.97	97						1	1	1	0	1	1	1	0	**16**	0	1	0	0
905-168	245528	2231836	2134	Lucerito	DDH-LC-15	1.85	21						1	1	1	0	1	1	1	0	**16**	0	1	0	0
1305-236	245711	2231589	2289	Lucerito	Lucero Mine	1.96	14	2.5	30	2.5	15	3	0	0	1	0	1	0	1	0	**7**	0	1	0	0
1301-31	245955	2231430	2335	Karina	Surface	0.01	0.5	17	5	52	20	0.5	1	1	1	0	0	1	1	0	**13**	0	1	0	0
1305-230	245814	2231686	2300	Karina	Karina Mine	0.29	49	8	5	6	60	16	0	0	1	0	1	1	1	0	**8**	0	1	1	0
1305-230A	245814	2231686	2300	Karina	Karina Mine	0.44	48	13	210	8	174	17	1	0	1	0	0	1	1	0	**10**	0	1	0	0
1305-232	245906	2231595	2287	Karina	Karina Mine	0.62	178	36	5	18	100	24	1	0	1	0	1	0	1	0	**12**	0	1	0	0
1305-233	245868	2231649	2287	Karina	Karina Mine	0.41	132	2.5	20	6	63	28	0	0	1	0	0	0	1	0	**4**	0	1	0	0
1305-255	245864	2231487	2127	Karina	DN-1	0.59	131						0	0	1	0	1	0	1	0	**7**	1	1	0	0
1305-256	245862	2231486	2125	Karina	DN-1	0.11	2.5						1	0	1	0	1	0	1	0	**12**	0	1	0	0
1305-259	245927	2231533	2272	Karina	KA-15	1.27	337						0	0	1	0	1	0	1	0	**7**	1	1	0	0

(*continued on next page*)

Appendix A. (*continued*)

Sample Number	UTM X	UTM Y	Elevation (m)	Vein	Collection Location	Au (ppm)	Ag (ppm)	Cu (ppm)	Pb (ppm)	Zn (ppm)	As (ppm)	Sb (ppm)	LV	V	CT	BC	Ad	PT	JT	Gst	**BCF**	L + illite	Rhomb. Calcite	Comb Qtz	Zonal Tex. Qtz
1301-32	246115	2231422	2324	Daniela	Surface	0.06	57	13	5	15	11	0.5	1	1	1	0	0	1	1	0	**13**	0	0	0	0
1301-33	246170	2231399	2327	Daniela	Surface	0.60	254	8	5	25	5	0.5	0	0	1	0	0	0	1	0	**4**	0	0	0	0
1301-34	246743	2231044	2251	Daniela	Surface	0.01	8	5	5	13	48	0.5	1	1	1	1	0	1	1	0	**16**	0	1	0	0
1305-231	245925	2231599	2287	Daniela	Daniela Mine	1.07	71	5	70	2.5	14	9	0	0	1	0	1	1	1	0	**8**	0	1	0	0
1305-251	245978	2231556	2260	Daniela	DN-1	3.64	639						1	0	1	0	1	0	1	0	**12**	1	1	0	0
1305-252	245976	2231554	2257	Daniela	DN-1	9.45	326						0	0	1	0	1	0	1	0	**7**	0	1	0	0
1305-253	245976	2231554	2257	Daniela	DN-1	9.45	326						0	1	1	0	1	0	1	0	**10**	0	1	0	0
1305-254	245973	2231552	2254	Daniela	DN-1	21.10	755						1	1	1	0	1	1	1	0	**16**	1	1	0	0
1305-257	246002	2231570	2146	Daniela	DN-2	0.21	85						0	0	1	0	0	0	1	0	**4**	0	1	0	0
1305-258	246002	2231570	2144	Daniela	DN-2	0.13	22						0	0	1	0	1	1	1	0	**8**	0	1	0	0
1305-260	245974	2231561	2210	Daniela	KA-15	33.70	180						1	0	0	0	0	1	1	0	**7**	0	1	0	0
1305-261	245975	2231562	2209	Daniela	KA-15	3.60	232						1	0	1	0	0	0	1	0	**9**	0	1	0	0
1305-262	245976	2231562	2207	Daniela	KA-15	1.45	45						1	0	1	0	1	0	1	0	**12**	0	1	0	0
1105-198	249157	2231204	2301	Belen	Surface	1.84	232	37	10	26	160	62	1	0	1	0	1	0	1	0	**12**	0	0	0	0
905-118	245604	2231623	2266		DDH-LC-03	0.92	2.5						0	0	0	0	0	1	1	0	**2**	0	1	0	0
905-119	245604	2231622	2264		DDH-LC-03	0.24	8						1	0	0	0	0	1	1	0	**7**	0	1	0	0
905-120	245604	2231622	2257		DDH-LC-03	0.02	0.5	44	5	65	15	3	0	1	0	0	0	0	1	0	**4**	0	1	0	0
905-121	245602	2231621	2233		DDH-LC-03	1.06	6	155	5	51	22	2	1	1	0	0	0	0	0	0	**8**	0	1	0	0
905-122	245596	2231617	2154		DDH-LC-03	0.00	11						0	0	0	0	0	1	1	0	**2**	0	1	0	0
905-123	245594	2231616	2130		DDH-LC-03	0.00	2.5						0	0	1	0	0	1	1	0	**5**	0	1	0	0
905-128	245590	2231614	2078		DDH-LC-03	0.73	6						0	0	0	0	0	1	1	0	**2**	0	1	0	0
905-129	245337	2232027	2313		DDH-LC-26	0.24	7	51	5	45	70	2	0	1	0	0	0	0	1	0	**4**	0	1	0	0
905-130	245361	2232032	2269		DDH-LC-26	0.13	17						1	1	0	0	0	1	1	0	**10**	0	1	0	0
905-131	245364	2232032	2264		DDH-LC-26	0.00	0.5	51	5	54	4	1	0	0	0	0	0	1	1	0	**2**	0	1	0	0
905-132	245372	2232033	2251		DDH-LC-26	0.05	0.5	6	5	50	200	2	1	1	0	0	0	1	1	0	**10**	1	1	1	0
905-133	245379	2232035	2238		DDH-LC-26	0.96	54						0	0	0	0	0	0	1	0	**1**	0	1	0	0
905-134	245382	2232035	2232		DDH-LC-26	0.65	111	13	5	17	27	0.5	1	1	1	0	0	1	1	0	**13**	0	1	1	0
905-135	245391	2232037	2216		DDH-LC-26	1.47	189						1	0	1	0	1	0	1	0	**12**	0	0	0	0
905-136	245406	2232039	2191		DDH-LC-26	0.15	7	6	5	66	82	0.5	0	0	0	0	0	0	1	0	**1**	0	1	0	0
905-137	245425	2232043	2156		DDH-LC-26	3.82	65						0	0	0	0	0	0	1	0	**1**	0	0	0	0
905-138	245434	2232045	2140		DDH-LC-26	0.39	3	26	5	45	200	0.5	0	0	1	0	0	1	1	0	**5**	0	1	0	0
905-141	245450	2232047	2113		DDH-LC-26	3.91	34						1	0	1	0	1	0	1	0	**12**	0	1	0	0
905-142	245459	2232049	2097		DDH-LC-26	5.53	19						0	0	1	0	0	1	1	0	**5**	0	0	0	0
905-143	245483	2232053	2055		DDH-LC-26	0.06	1	30	5	18	100	0.5	0	0	0	0	0	1	1	0	**2**	0	1	0	0
905-144	245753	2231406	2240		DDH-LC-29	0.18	2.5						0	0	1	0	0	0	1	0	**4**	0	1	0	0
905-145	245754	2231411	2225		DDH-LC-29	0.00	14						0	0	0	0	0	0	1	0	**1**	0	0	1	0
905-146	245754	2231411	2225		DDH-LC-29	3.45	452						0	0	1	1	1	1	1	0	**11**	0	0	1	0
905-147	245755	2231427	2182		DDH-LC-29	0.08	0.5	27	5	71	161	0.5	0	0	0	0	0	0	1	0	**1**	0	1	0	0
905-149	245791	2231360	2306		DDH-LC-31	0.09	2	2.5	5	14	0.5	1	0	0	0	0	0	0	0	0	**0**	0	1	0	0
905-150	245808	2231361	2278		DDH-LC-31	0.03	0.5	10	5	30	47	0.5	0	0	0	0	0	0	1	0	**1**	0	1	0	0
905-151	245831	2231362	2240		DDH-LC-31	0.00	2.5						1	1	1	0	0	1	1	0	**13**	0	0	0	0
905-152	245843	2231362	2220		DDH-LC-31	0.04	0.5	10	5	58	90	0.5	0	0	0	0	0	0	0	0	**0**	0	0	0	0
905-154	245446	2231929	2263		DDH-LC-20	0.18	78	27	5	41	199	2	0	0	0	0	0	0	1	0	**1**	0	0	0	0
905-155	245453	2231930	2249		DDH-LC-20	0.71	275						1	1	1	0	0	1	1	0	**13**	1	1	0	0
905-156	245454	2231930	2247		DDH-LC-20	0.75	215						0	0	1	0	0	0	0	0	**3**	0	1	0	0
905-159	245499	2231937	2154		DDH-LC-20	6.40	501						0	0	1	0	1	1	1	0	**8**	0	0	0	0
905-160	245518	2231940	2114		DDH-LC-20	1.08	2.5						0	1	0	0	0	1	1	0	**5**	1	0	0	0
905-161	245519	2231940	2111		DDH-LC-20	0.00	2.5						0	0	0	0	1	1	1	0	**5**	0	1	0	0
905-162	245455	2231790	2302		DDH-LC-15	0.00	2.5						0	0	1	0	1	0	1	0	**7**	0	1	0	0
905-163	245456	2231791	2300		DDH-LC-15	0.83	42						1	0	1	0	0	1	1	0	**10**	0	1	0	0
905-164	245500	2231818	2200		DDH-LC-15	0.00	10						0	0	0	0	0	1	1	0	**2**	0	1	0	0
905-169	245536	2231841	2116		DDH-LC-15	0.35	2.5						0	0	1	0	0	1	1	0	**5**	0	1	0	0
1305-234	245834	2231671	2287	Other_Vein	Karina Mine	0.51	28	2.5	50	23	60	54	0	0	1	0	0	0	1	0	**4**	0	0	0	0
1305-235	245820	2231679	2287	Other_Vein	Karina Mine	0.23	36	5	5	26	220	14	0	1	0	0	1	0	1	0	**7**	0	1	0	0
0905186A	246621	2228369	2208	Other_Vein	Surface								1	1	1	0	0	1	1	0	**13**	0	0	0	0
1105-187	246656	2228389	2235	Other_Vein	Surface	0.03	0.5	13	0.5	7		4	0	0	0	0	0	0	0	0	**0**	0	0	0	0
1105-187	246657	2228389	2235	Other_Vein	Surface	0.04	2	11	0.5	19	41	3	0	0	0	0	0	1	1	0	**2**	0	1	0	0

Appendix A. (*continued*)

Sample Number	UTM X	UTM Y	Elevation (m)	Vein	Collection Location	Au (ppm)	Ag (ppm)	Cu (ppm)	Pb (ppm)	Zn (ppm)	As (ppm)	Sb (ppm)	LV	V	CT	BC	Ad	PT	JT	Gst	**BCF**	L + illite	Rhomb. Calcite	Comb Qtz	Zonal Tex. Qtz
Oct_2011_1056559	245056	2231438	2400	Between Plateros and Melladito	Surface	0.04	0.5	59	0.5	26	1	0.5	0	0	0	0	0	0	0	0	**0**	0	0	0	0
Oct_2011_1056560	245002	2231546	2421	Between Plateros and Melladito	Surface	0.01	0.5	61	0.5	19	0.5	0.5	1	1	0	0	0	0	0	0	**8**	0	0	0	0
Oct_2011_1056580	247119	2228983	2267	Other_Vein	Surface	0.16	26	6	0.5	11	55	8	0	0	0	0	0	0	1	0	**1**	0	1	0	0

Concentration of metals in ppm.
LV = coexisting liquid-rich and vapor-rich inclusions with a broad range in liquid-to-vapor ratios.
V = assemblages consisting of only vapor-rich inclusions.
CT = colloform texture.
BC = Bladed calcite or bladed.
Ad = Adularia.
PT = plumose texture.
JT = jigsaw texture.
Gst = Ghost-sphere quartz.
BCF = Boiling confidence factor.
L + illite = liquid-rich inclusions with trapped illite.
Rhomb. Calcite = Rhombohedral calcite.
Comb Qtz = comb texture.
Zonal Tex. Qtz = Zonal texture quartz.

References

Albinson, T., Norman, D.I., Cole, D., Chomiak, B., 2001. Controls on formation of low-sulfidation epithermal deposits in Mexico; constraints from fluid inclusion and stable isotope data. Special Publication (Society of Economic Geologists (U. S.)), 8, 1–32.

Albinson, T., Rubio, M.A., 2001. Mineralogic and thermal structure of the Zuloaga vein, San Martin de Bolanos district, Jalisco, Mexico. Special Publication (Society of Economic Geologists (U. S.)), 8, 115–132.

Baker, D., 2011. Geology and Structure Report on the San Ignacio Project Guanajuato, Mexico. Great Panther Silver Limted, p. 23. Unpublished report.

Blake, W.P., 1902. Notes on the mines and minerals of Guanajuato, Mex. Transactions of the Society of Mining Engineers of American Institute of Mining, Metallurgical and Petroleum Engineers, Incorporated (AIME), 216–223.

Bodnar, R.J., Lecumberri-Sanchez, P., Moncada, D., Steele-MacInnis, M., 2014. 13.5 – Fluid inclusions in hydrothermal ore deposits. In: Holland, H.D., Turekian, K.K. (Eds.), Treatise on Geochemistry. second ed. Elsevier, Oxford, pp. 119–142.

Bodnar, R.J., Reynolds, T.J., Kuehn, C.A., 1985. Fluid-inclusion systematics in epithermal systems. Rev. Econ. Geol. 2, 73–97.

Botsford, C.W., 1910. Geology of the Guanajuato District. Mexican Mining J., 30–33

Brown, K.L., 1986. Gold deposition from geothermal discharges in New Zealand. Econ. Geol. 81 (4), 979–983.

Browne, P.R.L., 1978. Hydrothermal alteration in active geothermal fields. Annu. Rev. Earth Planet. Sci. 6, 229–250.

Buchanan, L.J., 1979. The Las Torres Mine, Guanajuato, Mexico; ore controls of a fossil geothermal system, Colorado School of Mines, Colorado, pp. 138.

Buchanan, L.J., 1980. Ore controls of vertically stacked deposits, Guanajuato, Mexico. Am. Inst. Mining Eng., 26 Preprint 80-82.

Buchanan, L.J., 1981. Precious metal deposits associated with volcanic environments in the Southwest. Arizona Geol. Soc. Digest 14, 237–262.

Camprubi, A., Albinson, T., 2007. Epithermal deposits in Mexico; update of current knowledge, and an empirical reclassification. Special Paper – Geological Society of America, 422, 377–415.

Church, J.A., 1907a. The mines of La Luz, Guanajuato, Mexico. Eng. Mining J., 153–155

Church, J.A., 1907b. The Mines of La Luz, Guanajuato, Mexico II. Eng. Mining J., 105–110

Clark, J.R., Williams-Jones, A.E., 1990. Analogues of epithermal gold-silver deposition in geothermal well scales. Nature 346 (6285), 644–645.

Collins, P.L.F., 1979. Gas hydrates in CO_2-bearing fluid inclusions and the use of freezing data for estimation of salinity. Econ. Geol. 74 (6), 1435–1444.

Dong, G., Morrison, G., Jaireth, S., 1995. Quartz textures in epithermal veins, Queensland – classification, origin, and implication. Econ. Geol. 90, 1841–1856.

Goldstein, R.H., Reynolds, T.J., 1994. Systematics of fluid inclusions in diagenetic minerals: Society for Sedimentary Geology Short Course 31, 199 pp.

Gómez, d.l.R.E., 1963. Estudio geológico minero de la zona de La Luz, distrito de Guanajuato, Gto., Consejo de Recursos Naturales no Renovables, México D.F.

Gross, W.H., 1975. New ore discovery and source of silver-gold veins, Guanajuato, Mexico. Econ. Geol. 70 (7), 1175–1189.

Gunnarsson, I., Arnórsson, S., 2000. Amorphous silica solubility and the thermodynamic properties of $H_4SiO^\circ_4$ in the range of 0° to 350°C at Psat. Geochim. Cosmochim. Acta 64, 2295–2307.

Haas, J.L., 1971. The effect of salinity on the maximum thermal gradient of a hydrothermal system at hydrostatic pressure. Econ. Geol. 66 (6), 940–946.

Hedenquist, J.W., Henley, R.W., 1985a. Hydrothermal eruptions in the Waiotapu geothermal system, New Zealand; their origin, associated breccias, and relation to precious metal mineralization. Econ. Geol. 80 (6), 1640–1668.

Hedenquist, J.W., Henley, R.W., 1985b. The importance of CO_2 on freezing point measurements of fluid inclusions: evidence from active geothermal systems and implications for epithermal ore deposition. Econ. Geol. 80, 1379–1406.

Hedenquist, J.W., Lowenstern, J.B., 1994. The role of magmas in the formation of hydrothermal ore deposits. Nature 370 (6490), 519–527.

Hedenquist, J.W., Arribas, A., Eliseo, G.-U., 2000. Exploration for epithermal gold deposits. Soc. Econ. Geol. Rev. 13, 245–277.

Henley, R.W., 1985. The Geothermal framework for epithermal deposits. Rev. Econ. Geol. 2, 1–24.

Henley, R.W., Brown, K.L., 1985. A practical guide to the thermodynamics of geothermal fluids and hydrothermal ore deposits. Rev. Econ. Geol. 2, 25–44.

Kamilli, R.J., Ohmoto, H., 1977. Paragenesis, zoning fluid inclusions, stable isotopic studies of the Finlandia Vein, Colqui District, Central Peru. Econ. Geol. 72, 950–982.

Lewis, W.J., Murahwi, C.Z., Leader, R.J., 2011. NI 43-101 Techical report audit of the resource and reserve estimates for the Guanajuato mines project Guanajuato state, Mexico, 172.

Mancano, D.P., Campbell, A.R., 1995. Microthermometry of enargite-hosted fluid inclusions from the Lepanto, Philippines, high-sulfidation CuAu deposit. Geochim. Cosmochim. Acta 59 (19), 3909–3916.

Mango, H.N., 1992. Origin of epithermal Ag-Au-Cu-Pb-Zn mineralization on the Veta Madre, Guanajuato, Mexico, Dartmouth College, Hanover, New Hampshire, 216 pp.

Martin, P.F., 1906. Mexico's Treasure House (Guanajuato): An Illustrated and Descriptive Account of the Mines and Their Operations in 1906. Cheltenham Press, New York. 259, ix pp..

Moncada, D., Bodnar, R.J., 2012a. Fluid inclusions and mineral textures of samples from the San Ignacio project, Guanajuato, Mexico. Great Panther Silver Limted, Unpublished report, pp. 27.
Moncada, D., Bodnar, R.J., 2012b. Identification of target areas for exploration in the La Luz area, Guanajuato, Mexico, based on fluid inclusions and mineral textures. Endeavour Silver Corp., Unpublished report, pp. 29.
Moncada, D., Bodnar, R.J., 2012c. Gangue mineral textures and fluid inclusion characteristics of the Santa Margarita Vein in the Guanajuato Mining District, Mexico. Central Eur. J. Geosci. 4 (2), 300–309.
Moncada, D., Mutchler, S., Nieto, A., Reynolds, T.J., Rimstidt, J.D., Bodnar, R.J., 2012. Mineral textures and fluid inclusion petrography of the epithermal Ag–Au deposits at Guanajuato, Mexico: application to exploration. J. Geochem. Explor. 114, 20–35.
Nieto-Samaniego, A.F., Alaniz Alvarez, S.A., Camprubi Cano, A., 2005. La Mesa Central de México: estratigrafía, estructura y evolución tectónica cenozoica. Bol. Soc. Geol. Mex. 57 (3), 285–317.
Person, M., Banerjee, A., Hofstra, A., Sweetkind, D., Gao, Y., 2008. Hydrologic models of modern and fossil geothermal systems in the Great Basin: Genetic implications for epithermal Au-Ag and Carlin-type gold deposits. Geosphere 4, 888–917.
Pokrovski, G.S., Akinfiev, N.N., Borisova, A.Y., Zotov, A.V., Kouzmanov, K., 2014. Gold speciation and transport in geological fluids: insights from experiments and physical-chemical modelling. Geol. Soc., London, Spec. Publ. 402 (1), 9–70.
Rowland, J.V., Simmons, S.F., 2012. Hydrologic, magmatic, and tectonic controls on hydrothermal flow, Taupo Volcanic Zone, New Zealand: implications for the formation of epithermal vein deposits. Econ. Geol. 107, 427–457.
Sander, M.V., Black, J.E., 1988. Crystallization and recrystallization of growth-zoned vein quartz crystals from epithermal systems; implications for fluid inclusion studies. Econ. Geol. 83, 1052–1060.
Saunders, J.A., Hofstra, A.H., Goldfarb, R.J., Reed, M.H., 2014. 13.15 – Geochemistry of hydrothermal gold deposits. In: Turekian, H.D.H.K. (Ed.), Treatise on Geochemistry. second ed. Elsevier, Oxford, pp. 383–424.
Shenberger, D.M., Barnes, H.L., 1989. Solubility of gold in aqueous sulfide solutions from 150 to 350 °C. Geochim. Cosmochim. Acta 53, 269–278.
Seward, T.M., Williams-Jones, A.E., Migdisov, A.A., 2014. 13.2 – The chemistry of metal transport and deposition by ore-forming hydrothermal fluids. In: Turekian, H.D.H.K. (Ed.), Treatise on Geochemistry. second ed. Elsevier, Oxford, pp. 29–57.
Simmons, S.F., Browne, P.R.L., 2000. Hydrothermal minerals and precious metals in the Broadlands-Ohaaki geothermal system: implications for understanding low-sulfidation epithermal environments. Econ. Geol. 95, 971–999.
Simmons, S.F., Christenson, B.W., 1994. Origin of calcite in a boiling geothermal system. Am. J. Sci. 294, 361–400.
Simmons, S.F., White, N.C., John, D.A., 2005. Geological Characteristics of Epithermal Precious and Base Metal Deposits. Economic Geology 100th Anniversary Volume, Economic Geology; One Hundredth Anniversary Volume, 1905–2005, 485–522.
Starling, T., 2008. Structural Review of the Deposits of the Northern Guanajuato District, Mexico, Field Visit Conclusions 03–08 prepared for Endeavour Silver Corp. Telluris Consulting, pp. 23.
Stefánsson, A., Seward, T.M., 2003. Experimental determination of the stability and stoichiometry of sulphide complexes of silver(I) in hydrothermal solutions to 400 °C. Geochim. Cosmochim. Acta 67 (7), 1395–1413.
Stefánsson, A., Seward, T.M., 2004. Gold(I) complexing in aqueous sulphide solutions to 500 °C at 500 bar. Geochim. Cosmochim. Acta 68 (20), 4121–4143.
Sterner, S.M., Bodnar, R.J., 1984. Synthetic fluid inclusions in natural quartz; 1, Compositional types synthesized and applications to experimental geochemistry. Geochim. Cosmochim. Acta 48 (12), 2659–2668.
Vasallo, L.F., Reyes-Salas, M., 2007. Selenian polybasite from the Guanajuato Mining District. México Bol-e 3 (2), 1–16.
Velazquez, P., 1973. A Study of the Possibility that the Luz Mineral Camp of Guanajuato can be a Resurgent Producer of Silver and Gold. University of Guanajuato, Guanajuato.
Vikre, P.G., 1985. Precious metal vein systems in the National District, Humboldt County, Nevada. Econ. Geol. 80 (2), 360–393.
Waldegger, M.F., 2012. Techical report on the San Ignacio project mineral resource Guanajuato state, Mexico pp. 50.
Ward, H.G., 1828. Mexico in 1827. Henry Colburn, London, London, p. 643.
White, N.C., Hedenquist, J.W., 1995. Epithermal gold deposits: styles, characteristics and exploration. Soc. Econ. Geol. Newsl. 23, 9–13.